Impact of model errors and signal to noise problem on the predictive skill of decadal forecast systems

Work Package:	2
Deliverable:	2.1
Due Date:	31.10.2024 (Month 24)
Submission Date:	31.10.2024 (Month 24)
Dissemination Level:	Public
Type:	Report
Responsible:	MPI-M
Author(s):	Daniela Matei (MPI-M),Katja Lohmann (MPI-M), Rashed Mahmood (DMI), Shuting Yang (DMI), Remy Bonnet (CNRS-CERFACS), Teresa Carmo Costa (BSC), Roberto Bilbao (BSC), Pablo Ortega (BSC), Noureddine Omrani (UiB), Noel Keenlyside (UiB), Wan-Ling Tseng (ASTW), Yi-Chi Wang (ASTW)

Funded by the European Union

Contents

1 Summary for Publication

In contrast to numerical weather prediction, climate predictions on seasonal to decadal time scales remain challenging, especially over land and with respect to extreme events. One goal of Impetus4Change is to close the gap between current skill of climate predictions and estimates of potential climate predictability. This deliverable aims to gain deeper understanding of the factors limiting current predictive skill as well as to develop a novel method to better correct systematic errors in climate predictions.

Specifically, we have conducted the following studies:

- We analysed the teleconnection between North Atlantic Oscillation (NAO) and surface temperature in reanalysis and then initialised climate prediction systems. We suggest that mis-representation of this relationship in the models could be one of the reasons contributing to degradation of prediction skill in initialised predictions on multi-annual timescales.
- We investigate the factors that can potentially explain the differences in predictive skill for the North Atlantic Ocean heat content and the relative role played by external forcings, using a large multi-model ensemble of decadal predictions and historical simulations.
- We investigate the relationship between the NAO, an important climate pattern, and cold surges in East Asia. The NAO influences atmospheric circulation across the Northern Hemisphere, and our analysis shows that during its negative phase, the NAO strengthens East Asia through - a system that brings cold air from the north. This results in more frequent cold surges reaching Taiwan. We will use this relationship to test how well current decadal climate prediction models can simulate the NAO's impact on East Asia's climate, with the goal of improving predictions of extreme cold events in East Asia for the next 10 years.
- We introduce a new bias correction method that is an adaptation of the Model Output Statistics (MOS) method - frequently used to remove biases in numerical weather predictions to multiannual forecasts. Predictions performed with the I4C climate prediction systems are used and two case studies are presented.
- We assess the record-strong marine heat wave observed in the subpolar North Atlantic in summer 2023 in a large ensemble of historical and future simulations and show that - due to a warming mean state of the subpolar North Atlantic - individual ensemble members can reproduce a subpolar marine heat wave, which matches the intensity of the observed heat wave, within the current decade.
- We assess the strength of the NAO in summer in climate change simulations and show that global warming increases the probability of summer NAO extremes and risks of associated severe weather events in Europe.
- In collaboration with the University of Kiel, we assess European summer heat waves in low- and high-resolution versions of various climate models and show that the high-resolution model versions reduce model biases in the North

Atlantic and thus more realistically simulate European summer heat waves and their atmospheric precursors.

- We investigate the coupled multidecadal variability between the atmosphere and ocean in the North Atlantic, focusing on the NAO, the Atlantic Meridional Overturning Circulation (AMOC), and the Atlantic Multidecadal Variability (AMV). Using a conceptual model and set of model experiments, we show that internal variability primarily drives this oscillation, while external forcings like volcanic and solar activities modify its timing without altering the core feedback mechanisms. The study has implications on decadal climate predictions.
- We examine the influence of Cloud Radiative Effects (CREs) on Euro-Atlantic atmospheric blocking over the Euro-Atlantic sector using the so-called cloud-locking technique. We conducted three experiments: Control (CTL) realistic experiment. Cloud-Locking (CLOCK) disabling cloud-radiation feedback, and Longwave Off (LWOFF) removing longwave cloud radiative effects (see details below). Our results show that CREs significantly enhance blocking frequency, with LWOFF reducing it further by 37.3%. Improving CRE representation in models, especially by transitioning to cloud-resolving models, could enhance blocking predictions.
- We examined how the tropical ocean warming (TOW) influences the future long-term projection of the Stratospheric Polar Night Jet (SPNJ), which strongly impacts the surface weather. It is shown that TOW controls the future SPNJ-response to climate change by increasing atmospheric wave activities and processes like diabatic heating and diffusive mixing. Therefore, biases in how models simulate tropical SSTs can reduce the accuracy of long-term climate predictions.

2 Contribution to the top-level objectives of Impetus4Change

2.1.1.1 **Objective**	2.1.1.2 **Contribution from Deliverable**
Overall Objective: to improve the quality, accessibility and usability of near-term climate information and services at local to regional scales – where impacts are most keenly felt and on-the ground adaptation is implemented – to strengthen and support end-user adaptation planning and action	By identifying factors degrading predictive skill based on state-of-the-art climate prediction systems as well as potential ways to enhance current predictive skill, this deliverable acts as the basis for improved quality of climate predictions on seasonal to decadal time scales as part of forthcoming deliverables.

1) Improve understanding and flow of climate information through knowledge networks;	N/A
2) Address persistent shortcomings to deliver seasonal to decadal predictions of improved quality;	By identifying factors degrading predictive skill based on state-of-the-art climate prediction systems as well as potential ways to enhance current predictive skill, this deliverable acts as the basis for improved quality of climate predictions on seasonal to decadal time scales as part of forthcoming deliverables.
3) Develop novel methods to downscale predictions to local scales;	N/A
4) Improve assessments of hazards and translate this into usable information for local risk assessments;	N/A
5) Make advances towards the goal of end-to-end seamless climate services;	N/A
6) Through transdisciplinary co-production approaches develop fit-for-purpose "Adaptation support packs" at municipal scales through our so-called urban Demonstrators;	N/A
7) Ensure high impact and visibility through robust and targeted communication and engagement;	N/A
8) Commit to Open Science through development of open access tools and exploitation of data/model outputs via relevant platforms thereby ensuring improved accessibility and usability of climate knowledge.	This deliverable is based on existing climate model simulations, largely from the sixth phase of the Coupled Model Intercomparison Project (CMIP6). Peer-reviewed publications related to this deliverable aim for open-access.

3 Detailed Report

3.1 Introduction

Current climate predictions on seasonal to decadal time scales continue to exhibit low skill, especially over land areas and with respect to climate extremes. One of Impetus4Change's fundamental science goals is to bridge the gap between predictive skill of state-of-the-art climate predictions and estimates of potential climate predictability. Within the framework of this deliverable, we have analysed existing simulations [mainly historical and decadal prediction experiments from the sixth phase of the Coupled Model Intercomparison Project (CMIP6) as well as from

Grand Ensembles performed with climate models of Impetus4Change partners] to better understand factors degrading predictive skill in state-of-the-art climate predictions on seasonal to decadal time scales.

3.2 Work Carried Out

1) Teleconnection pattern of the North Atlantic Oscillation [DMI]

In this work we explore model discrepancies in simulating the observed teleconnection patterns between the North Atlantic Oscillation (NAO) and the surface air temperature, and its impact on decadal predictions of Eurasian climate. For this, we used sea level pressure and surface air temperature data from 10 different initialised prediction systems. We first analysed the skill of these prediction systems in predicting winter surface air temperature over Eurasia for two forecast periods. We find some added value from initialization, compared to the uninitialized ensemble mean, over Eurasia for the first winter forecasts (FY-1-1; Figure DMI_1). Generally, the CanESM5 model stands out in terms of widespread added value over Eurasia while some other models also seem to have positive values over eastern parts of Eurasia. However, we did not find appreciable widespread added value for the five year mean winter temperature forecasts (FY1-5) in any of the ten climate prediction systems though some models show added values over a limited region in eastern Eurasia. The reasons for the degradation of skill over time in initialised predictions have been documented in many previous studies. These include model discrepancies in representing the observed climate, initial shock due to differences in observed and model mean climate states and the climate drift after initialization (e.g. Bilbao et al., 2021).
Here we explore how the initialised prediction systems simulate the observed NAO and surface air temperature teleconnection during the winter season (Figures DMI_2 and DMI_3). The observed teleconnection between NAO and surface temperature over Eurasia is well known. The observed teleconnection patterns include negative correlation between NAO and surface temperature over Northern Canada, Greenland and northern Africa while positive correlation over Eurasia and Eastern United States (Figure DMI_2, top panel). Most initialised predictions are able to capture the observed patterns of NAO-temperature teleconnections, however, with some differences among the individual models in terms of spatial distributions of the correlations. The strength of the observed teleconnection is also underestimated by most prediction systems, as the positive/negative centres for the individual models are significantly weaker than the observed values. For the first winter forecasts (i.e. FY1-1), the teleconnection patterns are relatively better predicted by the CanESM5 model including large negative correlations over Northern Canada and Greenland and relatively stronger positive correlation over Eurasia. Interestingly the added value from initialization for CanESM5 is also positive and statistically significant (over several regions) suggesting that improving model simulations of NAO-temperature teleconnection is important for improved predictions of climate in the Eurasian region. This is also the case for FY1-5, where all models struggle to capture either the strength and/or the spatial distribution of the observed NAO-temperature teleconnection

(Figure DMI_3). These results suggest that although the initialised predictions may be skillful in predicting the observed NAO (e.g. Smith et al., 2020), however, the model simulations of its teleconnection with surface air temperature need to be improved in order to better predict the multi-year mean winter temperatures over Eurasia.

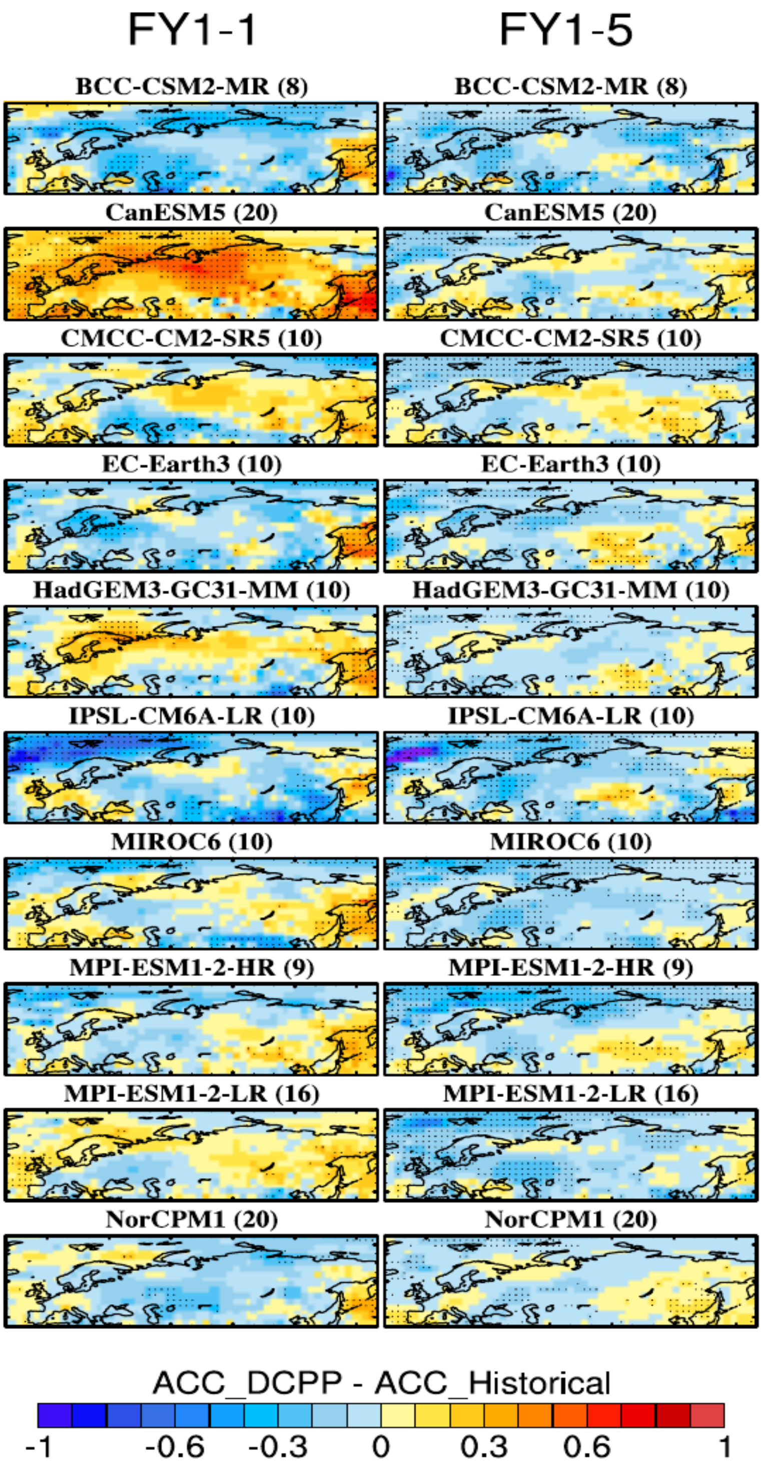

Figure DMI_1: Difference between the ACC of DCPP ensemble mean and ERA5 reanalysis from the ACC of historical ensemble mean and ERA5 for the surface air temperature of first winter season after initialization (left column) and average of first five winters (right column). Stipplings indicate regions where correlation differences are statistically significant at 90% confidence level. Note: Since some of the initialised predictions start from January, the first winter season forecast for DCPP is based on the average for months January and February. The DCPP ensemble sizes are shown in parentheses along with model names. Historical ensemble mean is based on 250 members from 30 different CMIP6 climate models. Observational data is from ERA5 reanalysis.

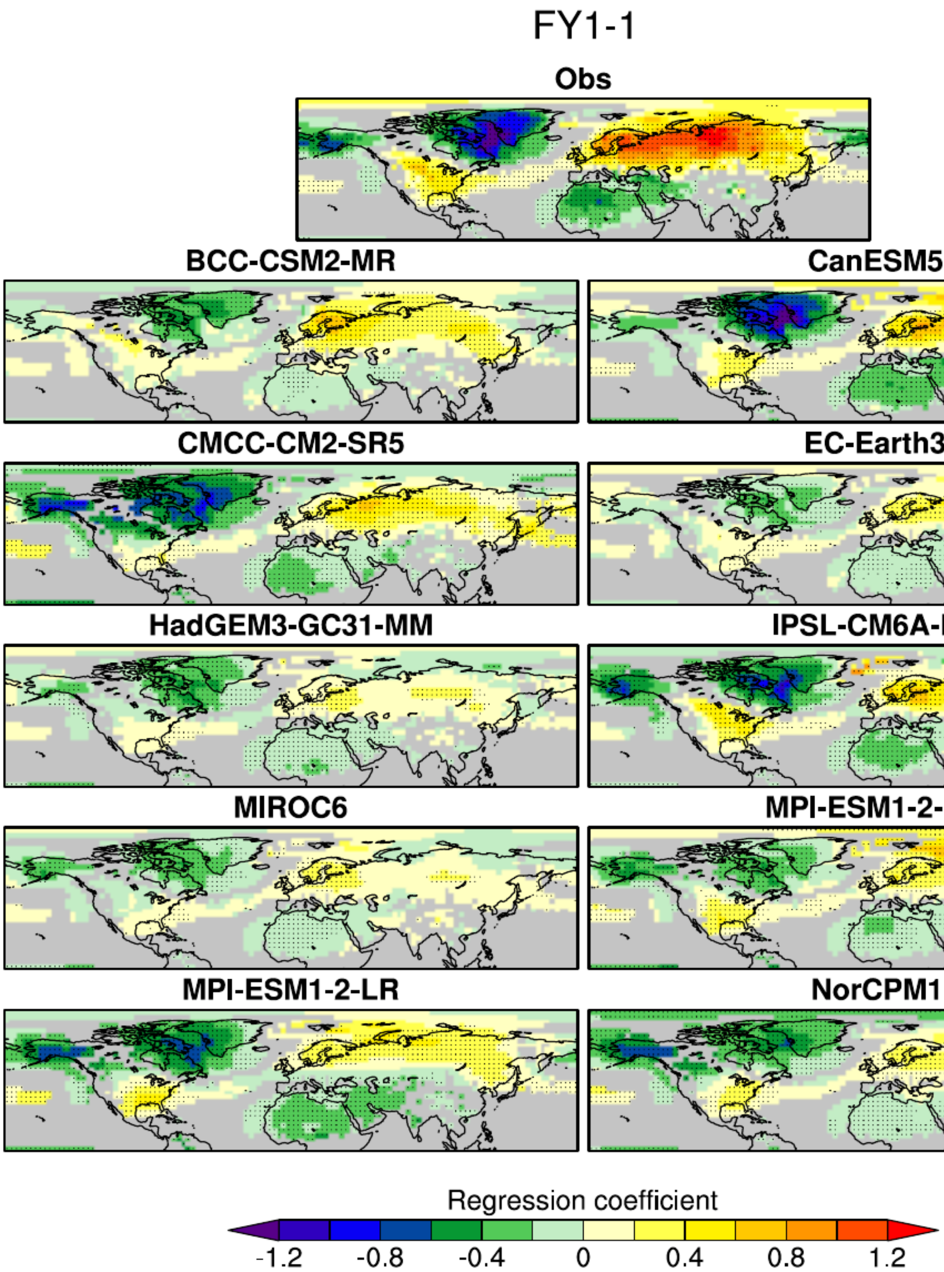

Figure DMI_2: Regression between the ensemble mean NAO and the surface air temperature for the first winter after initialization (for the period 1971-2010). The observed values less than 0.1 are set to missing for clarity. The model regression values are set to missing where observed regression is missing. Stipplings indicate regions where regression coefficient is statistically significant at 90% confidence level. The first row shows observed teleconnection patterns. Note: since some of the initialised predictions start from January, the first winter season forecast for the initialised predictions is based on the average for months January and February. Observational data is from ERA5 reanalysis.

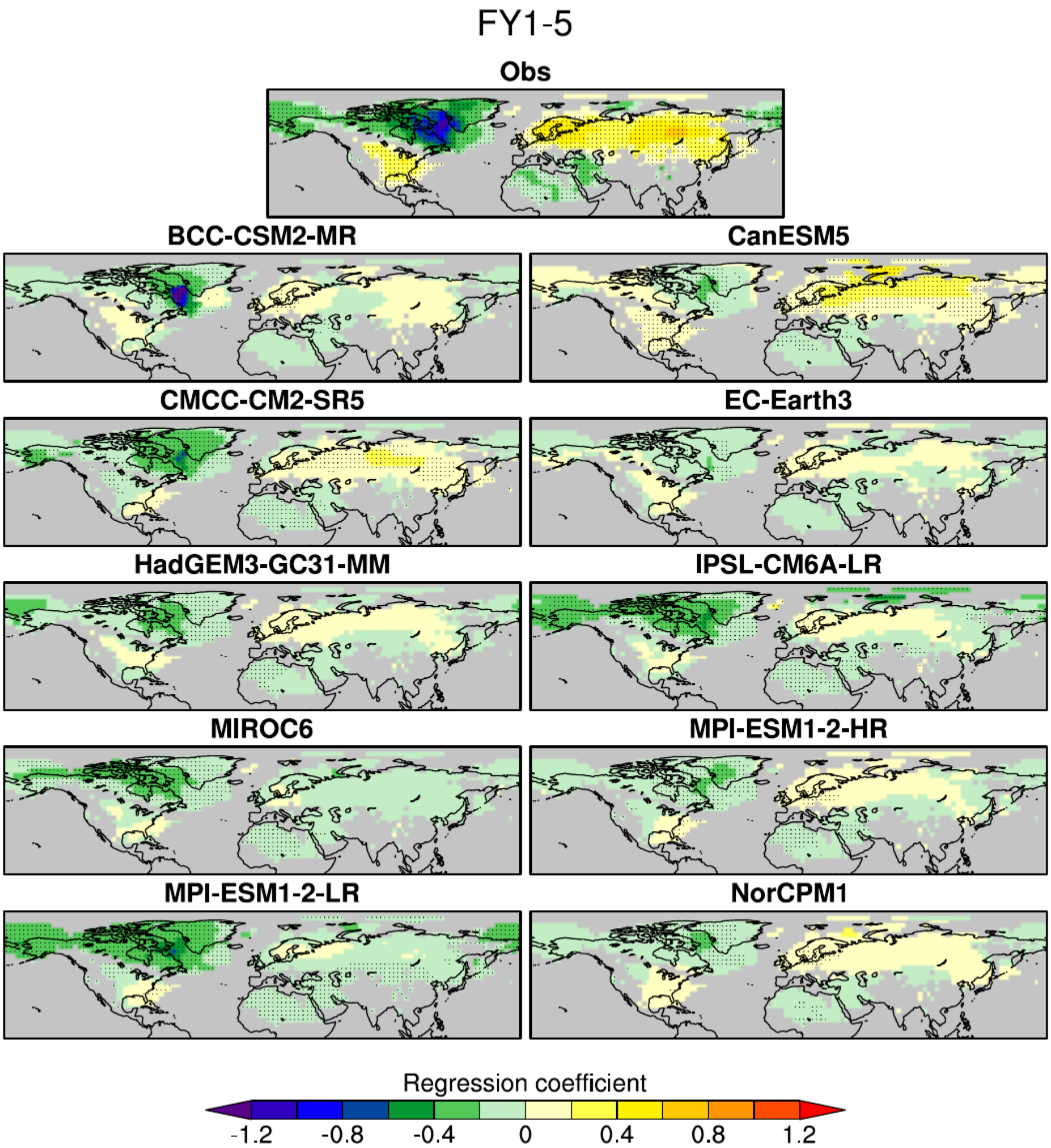

Figure DMI_3: Same as Figure DMI_2 but for 5 years mean winter forecasts.

2) Multi-model Analysis of the Factors Contributing to the Decadal Predictive skill of the North Atlantic Ocean Heat Content [BSC]

We have analysed eight CMIP6 climate models with comparable ensembles of decadal predictions and historical simulations to investigate their differences in predictive skill for the North Atlantic upper ocean heat content (OHC; defined as the integral in the upper 700 m) and to explore the predictive role of external forcings. Special attention was given to factors such as mean model biases, initialization approaches, and resolution, which could potentially explain the main multi-model differences in skill. These findings have been submitted to *Earth System Dynamics* (Carmo-Costa et al., in review).

The decadal predictions largely agree on regions with high predictive capacity for the OHC, primarily concentrating in the Labrador Sea region and the eastern flank of the North Atlantic (Figure BSC_1). All systems also show a region with negative skill scores in the middle of the Subpolar North Atlantic, although there are notable differences in the exact location and extent of the negative correlation values, which vary significantly across models and experiment types. Among these three regions, the largest inter-model differences occur in the Labrador Sea (in this study defined by the boundary coordinates 60-30°W and 45-65°N), where some models, like CanESM and IPSL, experience initial shocks, degrading the skill a few years after initialization. In this region, no clear consensus emerges from the multi-model ensemble regarding how much predictive capacity for the OHC is driven by external forcings, as large inter-model differences in correlation are found in the OHC of the HIST experiments (Figures BSC_1 and BSC_2). The added predictive value of initialization, determined by the difference in skill between the decadal predictions and historical ensembles, also varies greatly across models. This model-dependence underscores the importance of using multi-model approaches, as analyses focused on individual models, such as Carmo-Costa et al. (2022), can lead to misleading generalisations.

This study has not found a clear relationship between mean state biases in atmospheric forcing or local ocean stratification and decadal prediction skill (not shown). We attribute this to the fact that some of these biases are corrected through initialization, albeit differently depending on the initialization approach used. Full-field initialization (applied in four of the systems) directly improves the representation of those key model features in the first forecast years, including the vertical stratification and the surface forcing from the NAO, but this does not necessarily lead to systematic improvements in Labrador Sea OHC skill. No consistent benefit of anomaly initialization (applied in the other four systems) has been identified either. However, in the case of NorCPM1, we have found significant OHC skill throughout the entire forecast (Figure BSC_2), despite an overly weak mean stratification and some local errors in forced signals, demonstrating a beneficial effect of initialization.

Interestingly, in the historical experiments, we identified a strong linear relationship between Labrador Sea OHC skill and local density stratification, as well as a strong inverse linear relationship between skill and climatological local surface heat fluxes (Fig. BSC_3). Since both stronger stratification and weaker surface heat fluxes have a dampening effect on vertical mixing, we interpret that models with higher OHC skill are those where deep mixing occurs only sporadically, reducing the impact of spurious signals arising from internal variability, which tend to lower correlation values. Historical experiments with higher OHC skill in the Labrador Sea also exhibit larger biases in mean state stratification and heat fluxes, which raises questions about their realism. The multi-model mean of the historical experiments compares particularly well with observations and likely provides a more realistic estimate of predictability attributable to forcings. According to the multi-model mean, external forcings would account for 25% of the total OHC variance in the Labrador Sea.

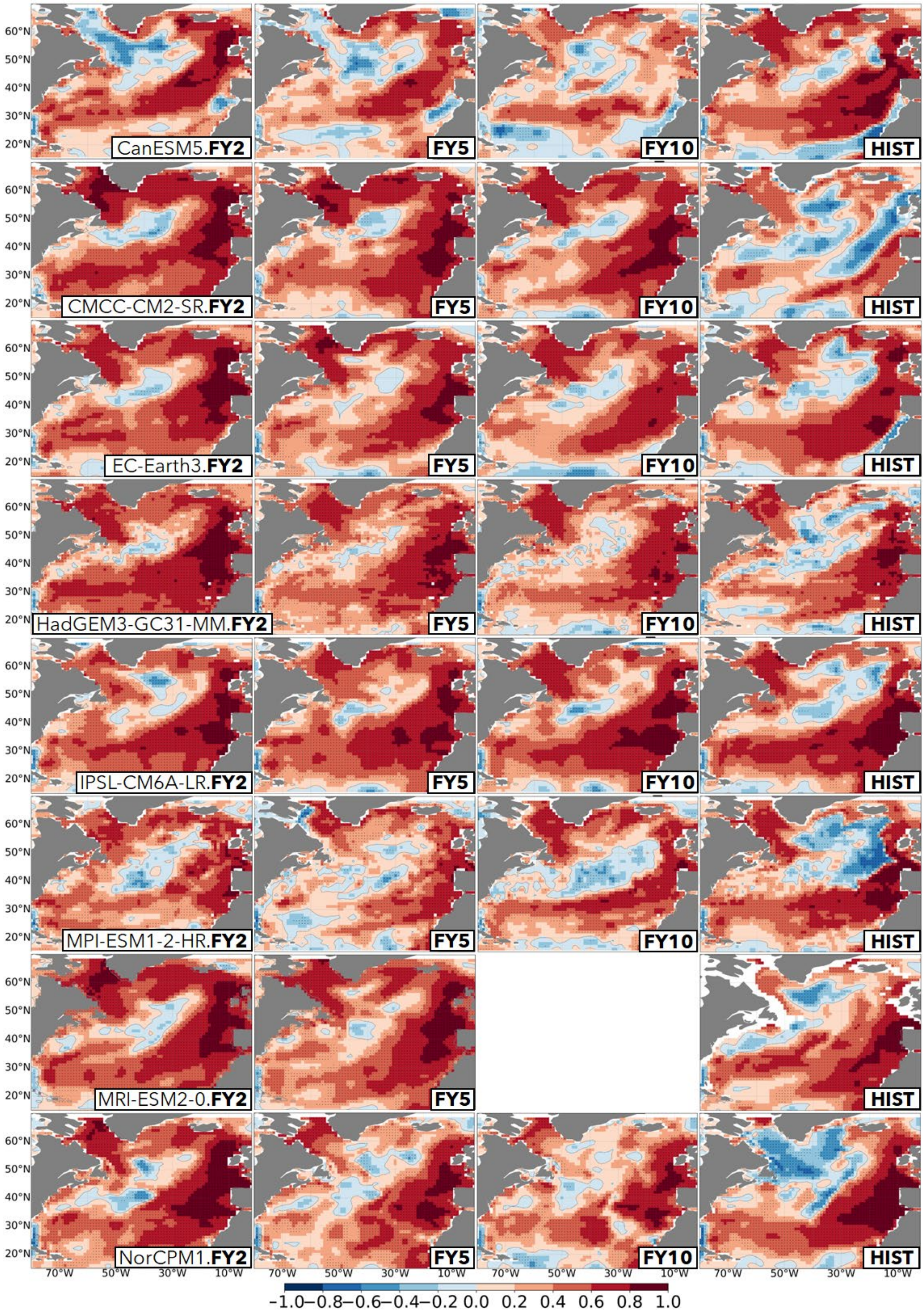

Figure BSC_1: Maps of anomaly correlation for the OHC in the DCPP (forecast years 2, 5 and 10; columns 1-3, respectively) and HIST ensembles (column 4). Stippling indicates cells with correlation values *statistically significant at the 95% confidence level. All correlation values are evaluated against EN4 for the period 1970-20.*

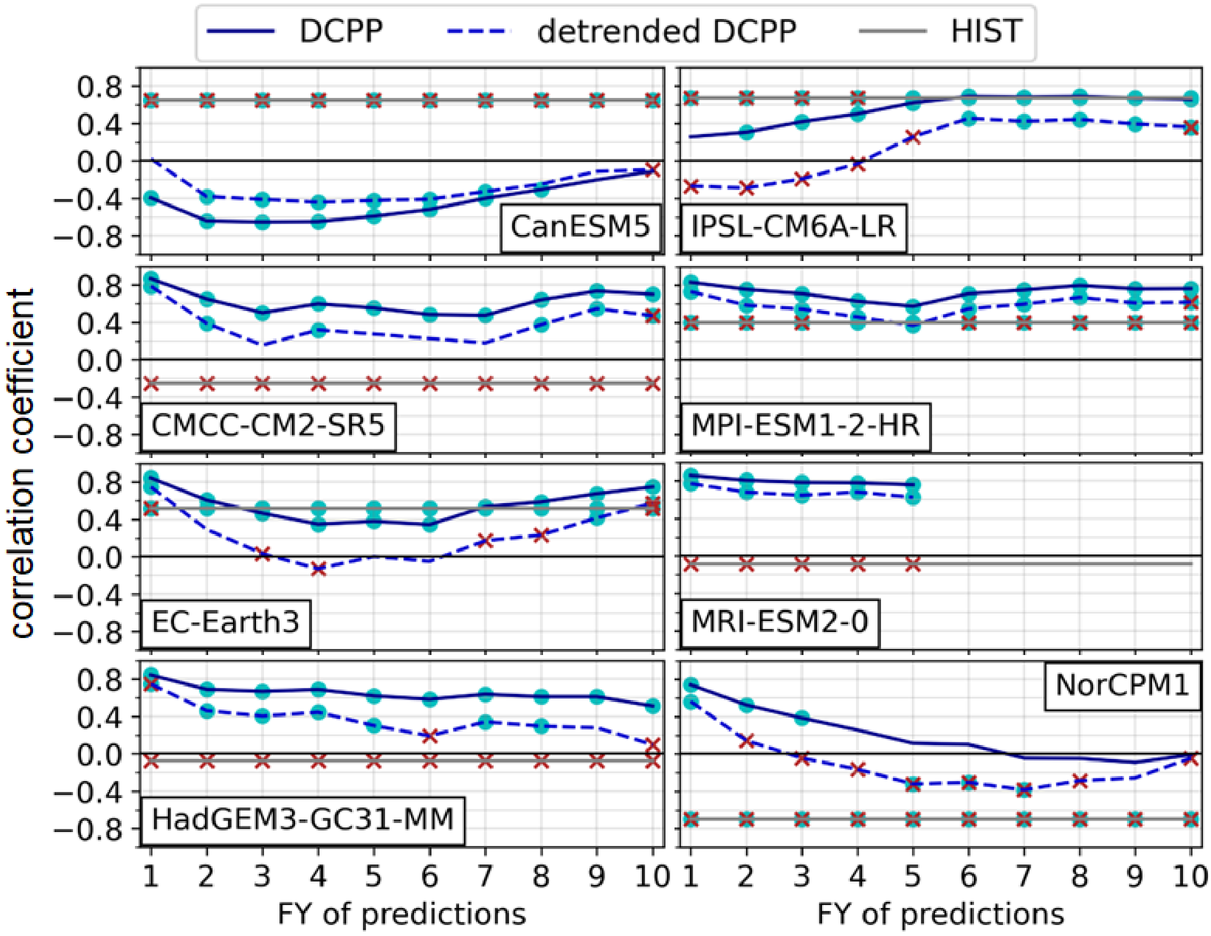

Figure BSC_2: Multi-model skill assessment of the OHC in the Labrador Sea region. Anomaly Correlation values are shown for the DCPP and HIST ensembles and evaluated against EN4 observations. In DCPP, skill is also computed after detrending both the forecast anomalies Cyan dots indicate ACC values that are significantly different from zero at the 95% confidence level. Red crosses indicate that the HIST or the detrended DCPP ACC values are significantly different from the DCPP values.

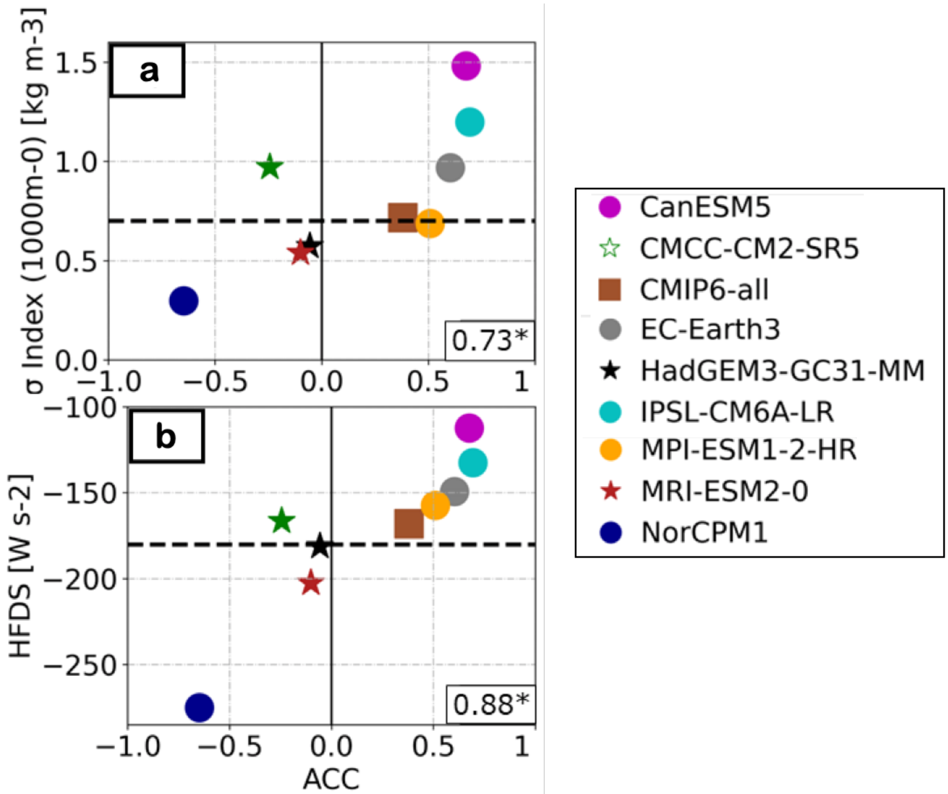

Figure BSC_3: (a) Scatterplot of the relationship between the predictive skill in the Labrador Sea OHC (horizontal axis) and the climatological value of index of the Labrador Sea density stratification in the HIST ensembles (vertical axis). The stratification index is computed as the density difference between 1000m and the surface. (b) The same as in (a) but between the predictive skill in the Labrador Sea OHC and the regressed values of the NAO index onto the Labrador Sea net surface heat fluxes in DJF (vertical axis). In all panels, stars represent non-significant correlation values at the 95% confidence level. The reference value from observations (EN4 in (a), ERA5 in (b)) is represented by the black dashed horizontal line. The correlation between the different pairs of metrics in the model space is shown for each plot in the lower right corners, with asterisks indicating if the correlation coefficient is significant at the 95% confidence level.

3) Skillful decadal predictability of cold surge frequency in Taiwan through North Atlantic Oscillation [ASTW]

The NAO has long been recognized as a key mode of climate variability, particularly for its role in decadal climate prediction over Europe (Smith et al., 2020). In this study, we evaluate the decadal prediction skill for cold surges in Taiwan, emphasizing the NAO's teleconnection with East Asia and its potential to improve decadal forecasting accuracy. Our work builds on the findings of Hong et al. (2008), who demonstrated that cold surge occurrences over Taiwan increase during the negative phase of the NAO and decrease during its positive phase. Extending their analysis through 2020, we present a 7-year running mean of anomalies for three key climate variables from 1940: Cold Surge Frequency (CSF) Anomaly (blue line), NAO Index (red line), and East Asia Trough Index (EAT, defined as averaged Z500 from 30°-45°N, 125°-145°E; black line) (Figure ASTW_1). The results show a clear in-phase relationship between the NAO and the East Asia trough, and an out-of-phase relationship between the NAO and CSF over Taiwan. These strong correlations suggest that NAO-driven signals modulate the variability of the East Asia trough via teleconnections, which subsequently influence cold surge frequency over Taiwan as the trough intensifies and extends further south.

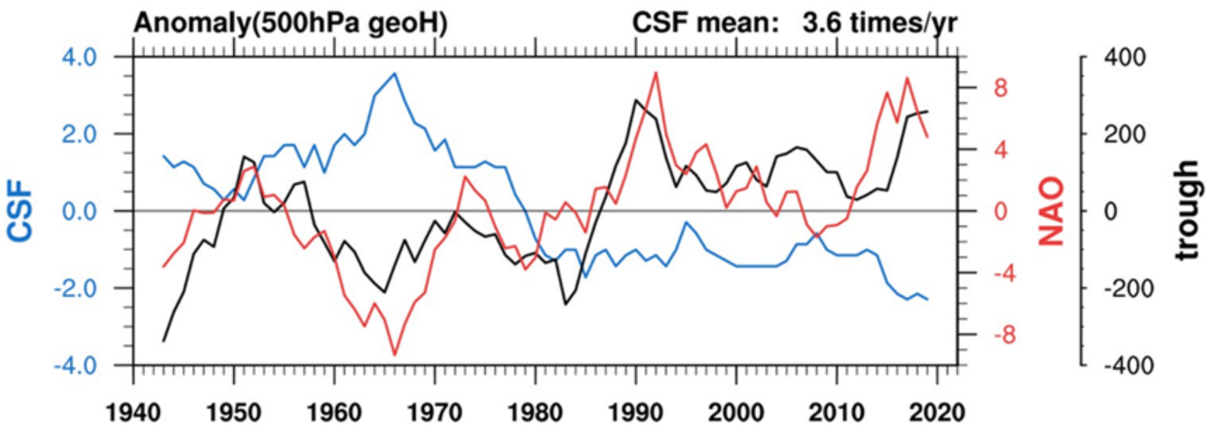

Figure ASTW_1: The 7-year running means of the CSF anomaly in Taiwan (blue bar), the NAO index (red bar) and the East Asia trough index (black line). The long-term mean CSF (3.6 times per year) was subtracted from the time series.

Figure ASTW_2 presents a composite analysis of atmospheric circulation patterns and wave activity flux at 200 hPa, illustrating the propagation pathway from the Atlantic to East Asia. Each panel displays snapshots taken 6, 4, and 2 days before, on the day of, and 2 days after the cold surge events, labelled as D-6, D-4, D-2, D0, and D2, respectively. These panels depict the evolution of wave patterns as they propagate eastward towards East Asia and eventually the central Pacific. Upon reaching East Asia, the associated wave activity flux facilitates the development of the East Asia trough, driving cold air outbreaks from high latitudes toward Taiwan. This analysis suggests that the NAO's teleconnection patterns, particularly during its negative phase, reinforce key atmospheric structures, such as the Siberian High, the ridge over Lake Baikal, and the East Asia trough - crucial elements for cold surge formation. Additionally, during the NAO's negative phase, reduced upper-level convergence over the Mediterranean-Sahara region promotes the formation of a wave-like atmospheric pattern that propagates toward East Asia via the subtropical jet stream, further enhancing cold surge events in the region.

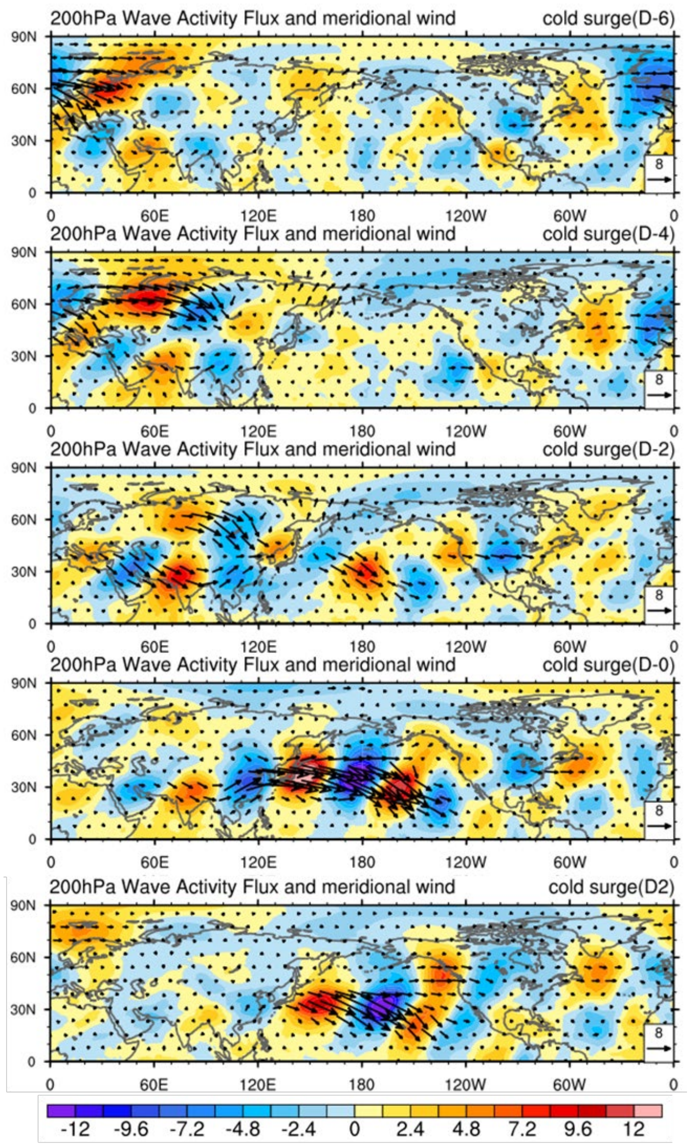

Figure ASTW_2: Circulation composite related to cold surge event anomalies in Taiwan. The graphic utilizes shading to indicate the streamfunction (106 m2 s-1) at 200 hPa and vectors to represent the wave activity flux (m2 s-2) at 200 hPa. The panels from top to bottom display the conditions -6 days, -4 days, -2 days, 0 days, and +2 days relative to the occurrence of a cold surge event.

Figure ASTW_3 focuses on the regional response around Taiwan. It reveals that during periods of increased cold surges in Taiwan, East Asia experiences overall colder temperatures, accompanied by a stronger East Asian trough (EAT) that transports cold air from higher latitudes (Figure ASTW_3a). This pattern aligns with the influence of the positive phase of the NAO, which is associated with colder temperatures across East Asia (Figure ASTW_3b). The relationship is further quantified through linear regression analysis, demonstrating a strong correlation between the EAT and CSF over Taiwan, as well as generally warmer winter temperatures in East Asia (Figure ASTW_3c, d). Our ongoing research aims to leverage this quantitative relationship between the NAO and CSF over Taiwan to assess the potential for decadal predictability of both winter mean temperatures and extreme cold events influenced by the NAO.

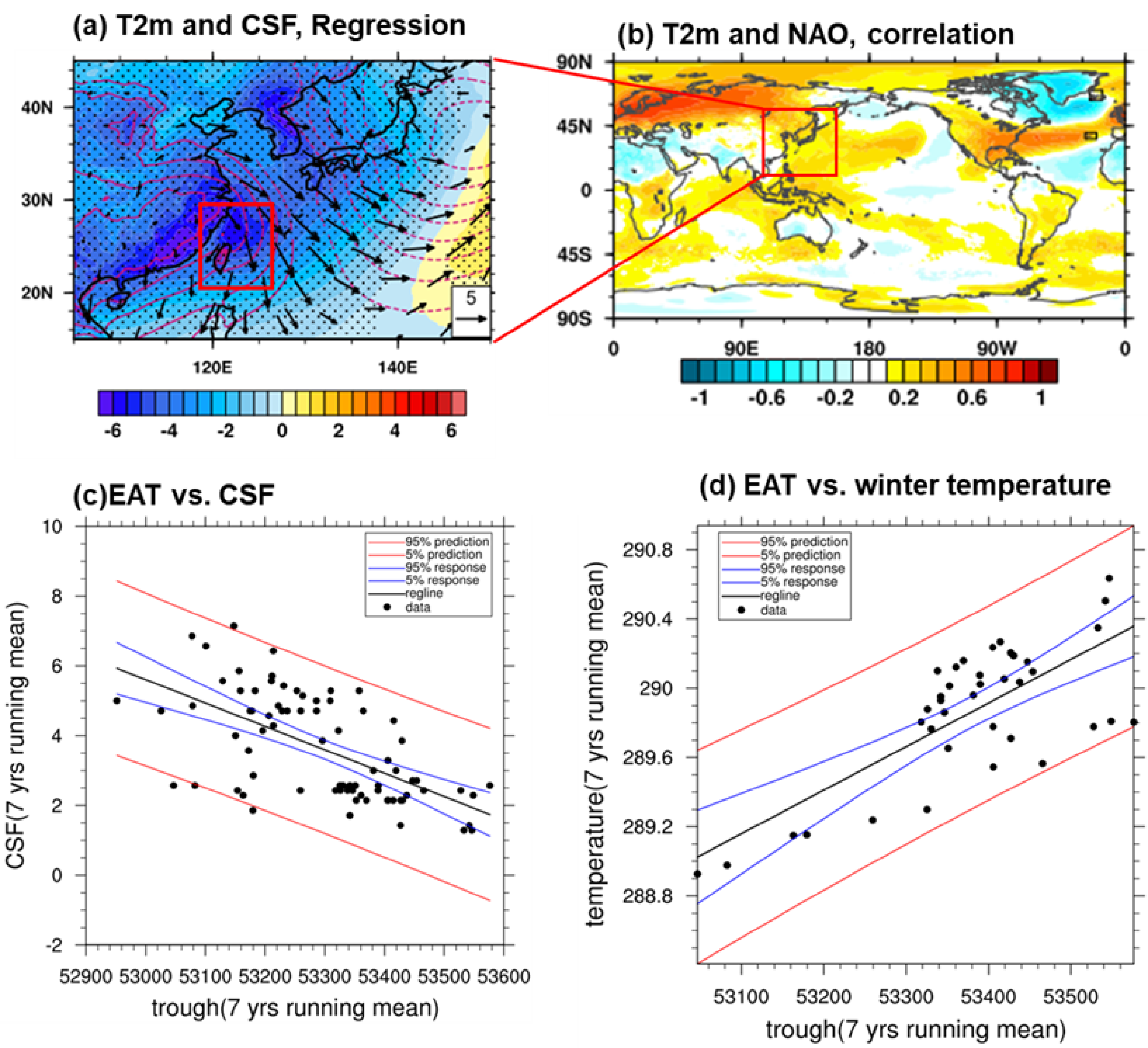

Figure ASTW_3: The upper panel demonstrates the circulation pattern related to cold surges in Taiwan and the NAO. (a) The regression map of 2m temperature (shading; °C) and 850 hPa wind (vector; m/s) onto the Cold Surge Frequency (CSF) over East Asia. (b) The correlation map of 2m temperature and the NAO index in the global domain. The lower panels show statistical relationships between the NAO index and CSF/winter temperature over a 7-year running mean. (c) The correlation between the EAT (x-axis, 7-year running mean) and the Cold Surge Frequency (CSF, y-axis), with data points (black dots) and predicted responses (lines) accompanied by the 95% and 5% prediction and response intervals. (d) Similarly, the relationship between the EAT and winter temperature (y-axis), following the same format with confidence intervals. The averaged domain is from the red box in (a).

4) New bias-correction method [CNRS-CERFACS]

Multiannual predictions performed with climate models suffer from initial shocks and drifts after the initialization that need to be corrected before forecast verification. Here we present a new bias correction method for climate predictions, based on the well-known Model Output Statistics (MOS) approach, which is widely used to correct bias in operational numerical weather predictions at Météo-France. MOS combines observational data from the target region or variable with forecast data using multiple linear regression (MLR) based-statistical model. Here, the idea is to adapt MOS to longer timescales to correct the drift and systematic errors in multiannual predictions produced by the I4C project. As mentioned above, MOS (Model Output Statistics) involves a Multiple Linear Regression (MLR) approach where the predictand is the observed variable "Y" over the region of interest. The predictors, denoted as X_n, include the forecasted variable over the same region and other forecast variables that are physically related to the target variable (see Figure CNRS-CERFACS_1). The goal is to determine the coefficients (β_n) for each predictor to reconstruct Y*, the bias-corrected predicted variable. It is important to note that a distinct MLR statistical model is developed for each lead time.

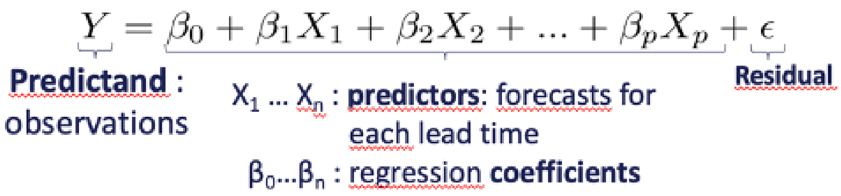

Figure CNRS-CERFACS_1 : Multiple linear regression implemented in the MOS bias correction method.

We have implemented a MOS drift correction using the interannual forecasts provided by the I4C global multiannual predictions systems based on the CNRM-ESM2.1, EC-Earth3 and NorCPM1 models. Predictions are performed by following the CMIP6/DCPP-A experimental protocol (Boer et al., 2016) for the forecast period 1960-2018. Two case studies are presented: the North Atlantic Sea surface temperatures (NASST), and the surface air temperature (SAT) over Europe. Lead times from 1 to 5 years are considered.

<u>(A) Bias correction of the North Atlantic SST (NASSTs)</u>

The target variable, NASST, is the annual means of SSTs spatially averaged over the North Atlantic north of 60ºN. The observations are issued from HadISST1 dataset. The predictors considered in this case study are the predicted NASSTs, the winter atmospheric patterns NAO, Blocking and Atlantic Ridge, and the number of years after a volcanic eruption. Winter atmospheric patterns have been determined from monthly sea level pressure data from ERA5 reanalysis for the same period: 1960 – 2018 by using EOFs analysis. Then the sea level pressure anomalies for the predictions for each model are projected over the ERA5 patterns to obtain the associated time series. The choice of the number of years after a volcanic eruption is motivated by the fact that the predictor needs to be gaussian to be considered in a MLR statistical model. Note that all the ensemble members are considered in the fit of the MLR model, and not the ensembles mean. The R2 coefficient indicates that the value of the explained variable of the MLR is above 50% for all the lead times and all the climate models (Figure CNRS-CERFACS_2a), indicating a good performance of the regression. We compare the bias correction achieved with MOS to the traditional bias correction provided by the WCRP, which consists in removing the mean systematic bias estimated from the multi-starting date, multi-member average over the forecast period. Figure CNRS-CERFACS_2b illustrates the comparison between the WCRP and MOS methods in terms of the Mean Squared Skill Score (MSSS). A MSSS score greater than 0 means that bias corrected forecasts with MOS are more accurate than those corrected by WCRP method. The results show that the MOS method performs better than the WCRP method for this specific case across all lead times, which is an important finding.

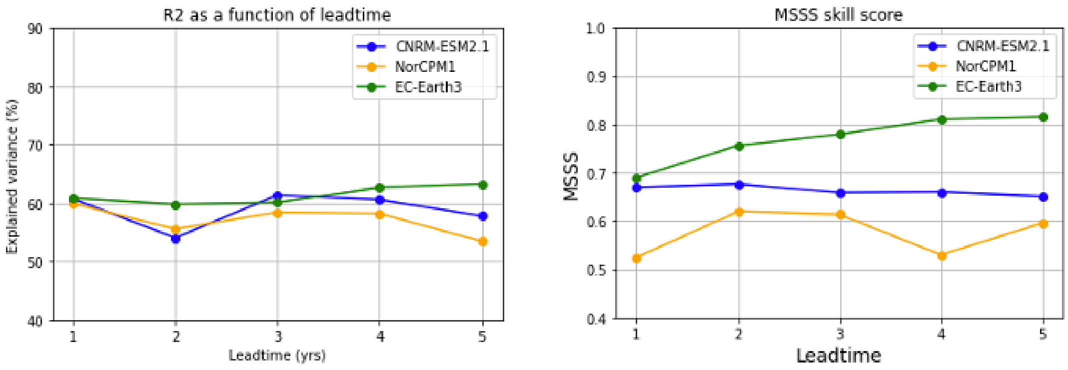

(a) (b)

Figure CNRS-CERFACS_2: (a) R2 (explained variance, %) of the MLR for each model. (b) MSSS score to compare MOS and WCRP bias and drift correction techniques as a function of lead time for the case study of NASST multiannual forecast.

Additionally, the MOS method allows us to quantify the relative contribution of each predictor to the reconstruction of the predictand (Figure CNRS-CERFACS_3). The greater contribution is associated with the NASST variable (more than 50%), followed by the atmospheric pattern's contribution. Interestingly, the results reveal that atmospheric patterns can contribute over 30% to the NASST reconstruction, which is a noteworthy finding. Note that volcanic eruptions contribute by 20%, which is not neglectable.

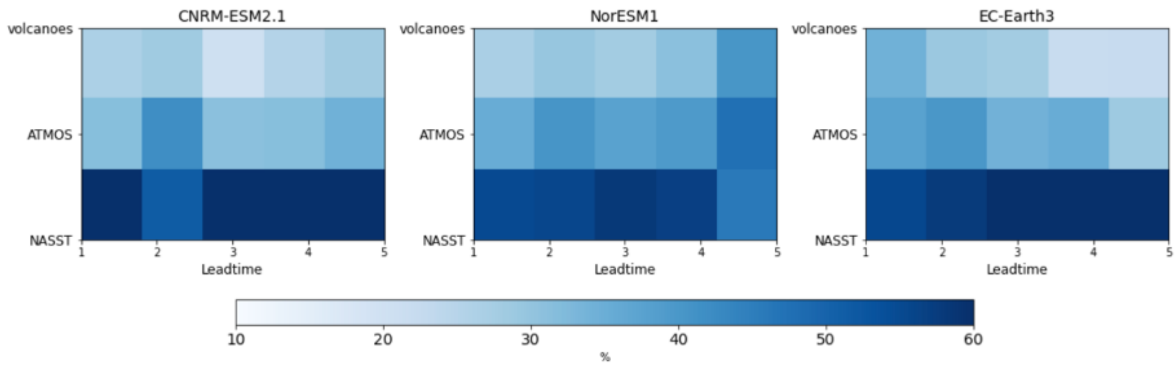

Figure CNRS-CERFACS_3: Relative contribution (%) of each predictor to the MLR fit to correct the bias of NASST predictions as a function of the lead time (in years). The predictors are: NASST forecasts, ATMOS (contribution of the three atmospheric patterns NAO, BL and AR) forecasts and the number of years after a volcanic eruption.

<u>(B) Bias correction of the European SAT</u>

In this particular case study, the annual SAT averaged over three climate regions identified in the AR6/IPCC report are considered: Northern Europe (NEU), Western and Central Europe (WCE), and Mediterranean (MED). In this case, the predictors (X_n) used for the MLR are the NASST predictions, the SAT predictions over the target region, the predictions of NAO, BL and AR atmospheric patterns and the number of years after a volcanic eruption. After the MLR fit, The R2 values show a good performance of the MLR model for the three regions (Figure CNRS-CERFACS_4).

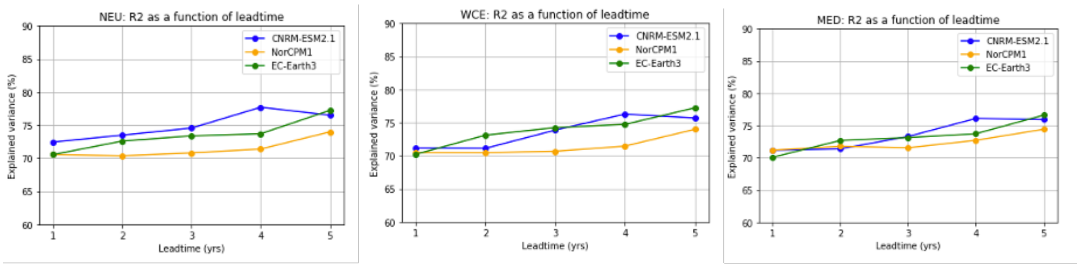

Figure CNRS-CERFACS_4: R2 (explained variance, %) of the MLR for each model for the SAT over the three different AR6 European regions: NEU, WCE and MED.

In terms of performance, SAT predictions corrected by MOS consistently show higher skill levels compared to those corrected by the traditional WCRP method (Figure CNRS-CERFACS_5), as indicated by positive MSSS values across all cases. It is worth noting that in the NEU region, the added value of MOS is more model-dependent, particularly for lead times greater than 3 years. Overall, MOS outperforms the WCRP method, especially in the MED region.

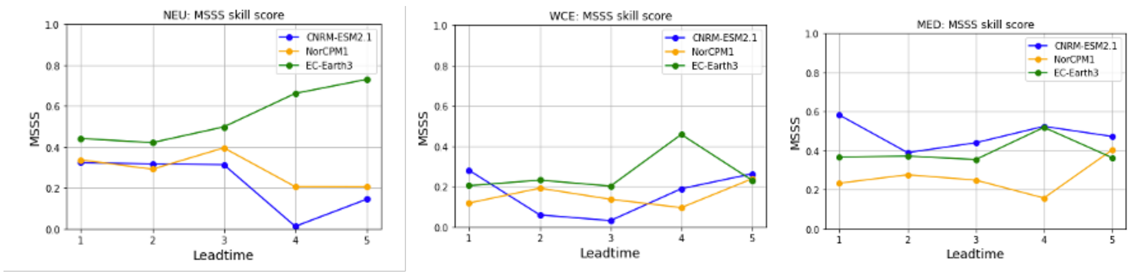

Figure CNRS-CERFACS_5: MSSS score to compare MOS and WCRP bias and drift correction techniques as a function of lead time for the case study of SAT multiannual forecast over the three European AR6 regions, NEU, WCE, MED.

To conclude, the analysis of the relative contribution of each predictor to the predicted SAT indicates that SAT forecasts contribute to a lesser extent to their own prediction. Other variables, such as NASST and atmospheric patterns, play a more significant role in this context. Atmospheric patterns are particularly important in the NorCPM1 model (Figure CNRS-CERFACS_6).

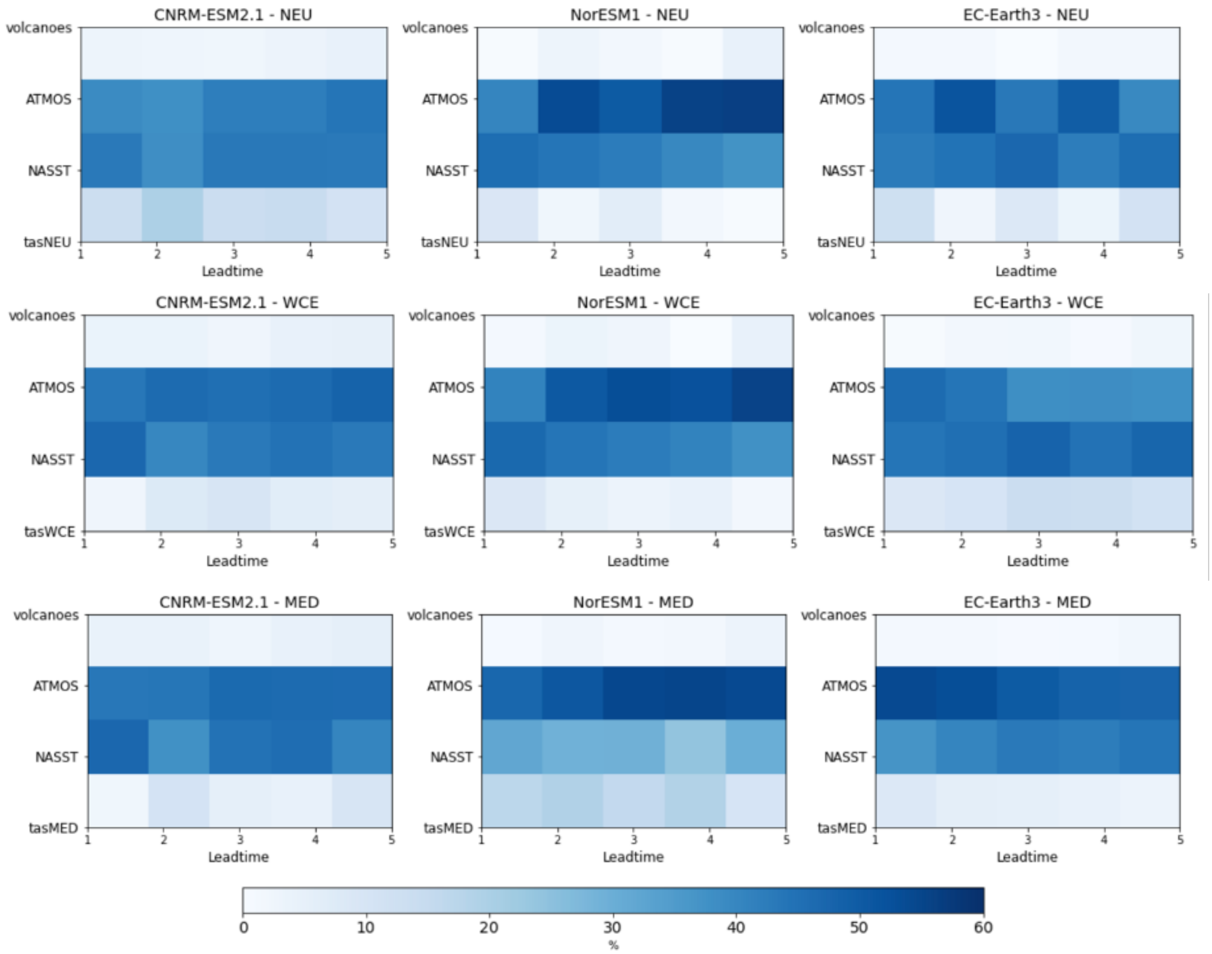

Figure CNRS-CERFACS_6: Relative contribution (%) of each predictor to the MLR fit to correct the bias of SAT predictions as a function of the lead time (in years) for the three AR6 climate regions: NEU, WCE and MED. The predictors are: SAT, NASST forecasts, ATMOS (contribution of the three atmospheric patterns NAO, BL and AR) forecasts and the number of years after a volcanic eruption.

In conclusion, we have presented an adaptation of the MOS method to correct errors in interannual predictions made with the three I4C forecast systems for two study cases. The uniqueness of this correction method is that it needs to be applied to each specific case, requiring knowledge of the physics involved to correctly select the predictors for the MLR model associated with MOS. This approach is particularly valuable for climate services. We have shown that MOS is effective, as predictions corrected with MOS exhibit higher predictive skill than those corrected with the traditional WCRP method. Furthermore, MOS is not only a correction method for forecast drifts; it also provides insights into the mechanisms of predictability.

5) The summer 2023 marine heat wave in the subpolar North Atlantic in the MPI-M Grand Ensemble [MPI-M]

A record-strong marine heat wave occurred in the subpolar North Atlantic in summer 2023 with spatially averaged sea surface temperature (SST) anomalies exceeding 1°C (red line in Figure MPIM_1). Based on analysis of historical/scenario simulations with different climate models (one realisation each, including the first member of the MPI-M Grand Ensemble), Kuhlbrodt et al. (2024) discuss the 2023 subpolar marine heat wave in the context of the expected mean climate change for various scenarios. Here, we extend the analysis of the MPI-M Grand Ensemble historical/scenario simulations to all 50 members and show that eight ensemble members simulate summer SST anomalies in the subpolar North Atlantic exceeding 1°C within the current decade (Figure MPIM_1, one ensemble member even in two adjacent summers). We underline that these eight ensemble members do not include the first member analysed by Kuhlbrodt et al. (2024). Considering the entire simulated period (1850-2100) indicates that the recent decades are a kind of transition phase, in which, due to a warming background state, subpolar marine heat waves as observed in summer 2023 may occur occasionally. Regarding potential drivers of the observed heat wave, our analysis of atmospheric reanalysis data suggests a large heat gain in the western subpolar North Atlantic in the winter of 2022/23, associated with a negative phase of the NAO in some of the winter months. All ensemble members reproducing the observed subpolar marine heat wave also simulate large subpolar surface heat gain in the respective preceding winter, though partly over different parts of the subpolar North Atlantic, related to the respective atmospheric winter circulation. For most of these ensemble members, an oceanic heat transport convergence across the subpolar gyre also contributes to the simulated subpolar marine heat wave. This study provides a basis for assessing the predictability of the 2023 subpolar marine heat wave with the MPI-M ocean-eddy resolving climate prediction system.

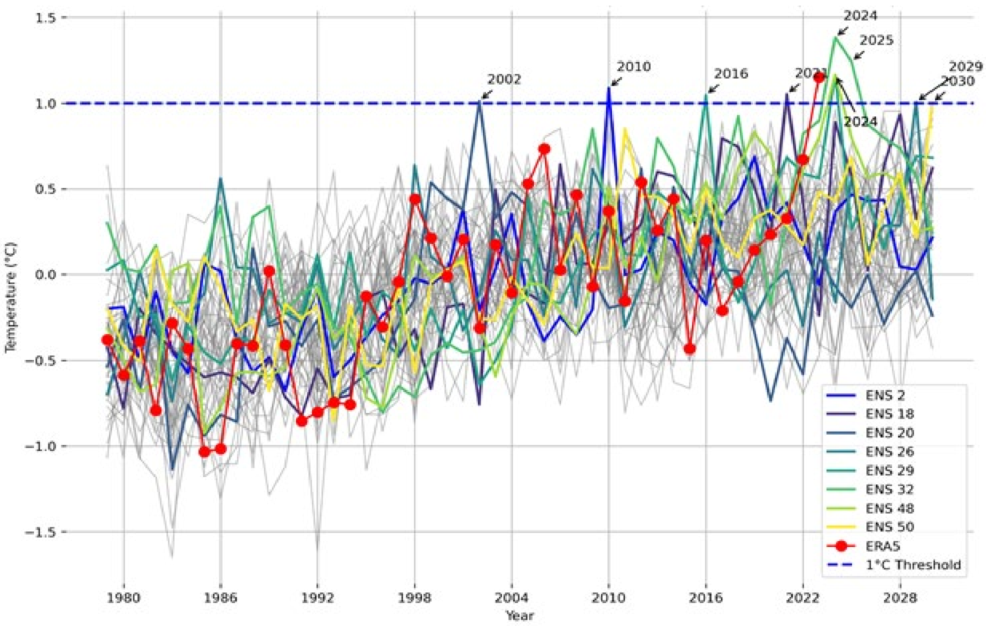

Figure MPIM_1: Sea surface temperature anomalies in summer (JJA) in the subpolar North Atlantic in atmospheric reanalysis (red line) and the MPI-M Grand Ensemble historical/scenario simulations.

6) More extreme summertime North Atlantic Oscillation under climate change [MPI-M]

Extreme states of the NAO in summer can lead to severe weather events such as heatwaves and floods in Europe. But how the summer NAO extremes evolve in response to climate change remains unexplored. Here we show that the statistical distribution of summer NAO index grows wider with increasing global warming in the MPI-M Grand Ensemble of climate change simulations as well as in reanalysis data. The amplified internal variability by global warming leads to a higher probability of internally generated summer NAO extremes - for both positive and negative phases - accompanied by an amplification of their impacts on surface temperature over northwestern Europe (Figure MPIM_2). This study highlights that global warming may degrade the predictive skill for the summer NAO by amplifying its internal variability, and thus exacerbate risks of the associated severe weather events in Europe.

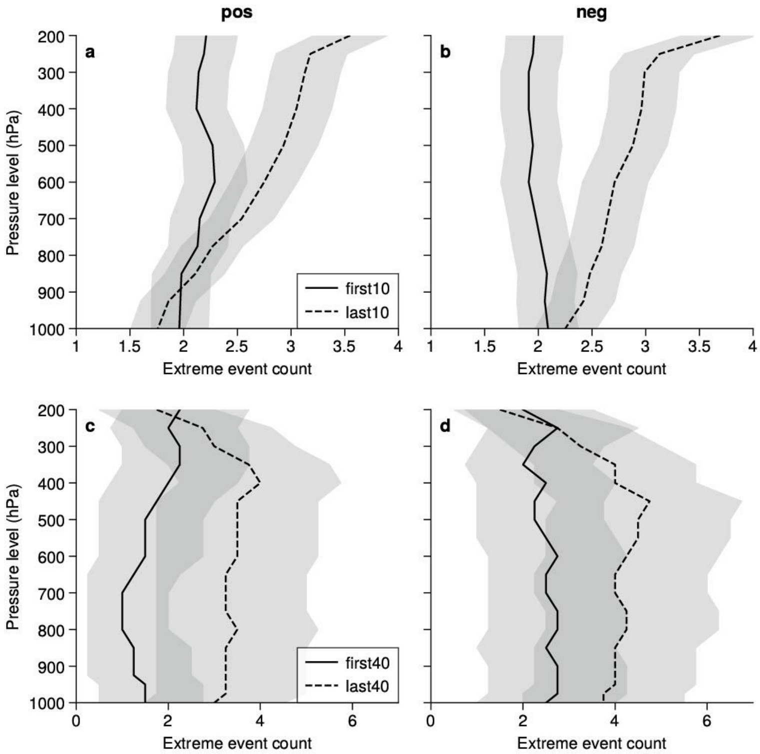

Figure MPIM_2: Profile of positive and negative summer NAO extremes in the first and last 10 years of the MPI-M Grand Ensemble 1%CO_2 simulations (upper panels) and in the first and last 40 years of the NOAA 20th Century Reanalysis (lower panels).

7) Improved European heat event simulation by resolving oceanic mesoscale eddies [University of Kiel with contributions from MPI-M]

Owing to the rapid increase of European heat event occurrences over the past decades, the understanding of their physical drivers has become increasingly important for the scientific community. Recently, it has been shown that cold North Atlantic sea surface temperatures (SSTs) are strongly linked to European heat events such as in summer 2015 and 2018. Thereby, an accurate representation of this connection in climate models is crucial for a more realistic European heat event simulation. Here, we investigate the connection by employing seven global coupled climate models, from which six models are embedded in the High Resolution Model Intercomparison Project (HighResMIP). High-resolution versions of these models capture mesoscale eddies, thus enabling study their impact on the North Atlantic SST - European summer temperature extremes connection. Our results show that high-resolution model versions better capture the North Atlantic trough and the downstream ridge anomalies over central Europe, although still underestimated in intensity and duration compared to observations (Figure MPIM_3). Improvements in high-resolution configurations are due to the increased ocean model resolution, which reduces the North Atlantic surface biases and improves air-sea interactions, thus having implications for the prediction and projection of climate extremes in the North Atlantic - European region.

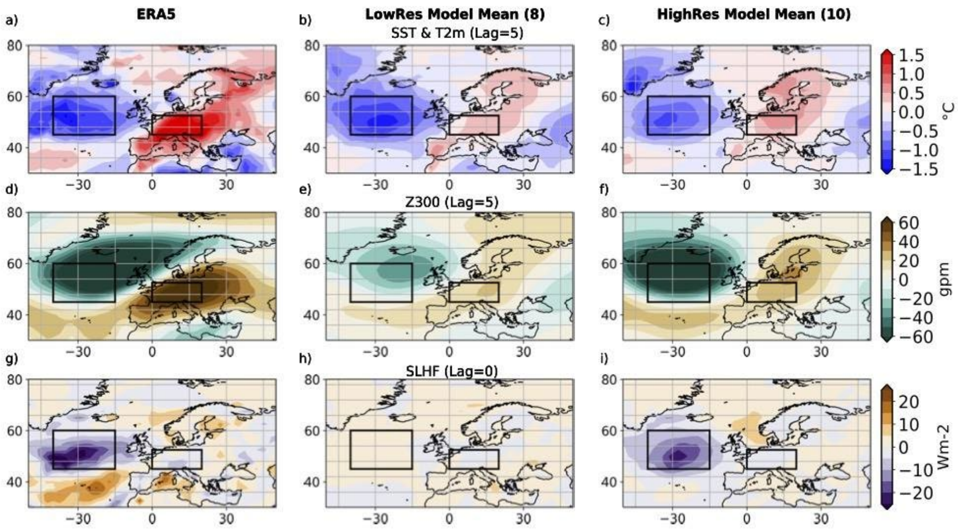

Figure MPIM_3: Composite-mean anomalies of 2-metre air temperature (upper panels), 300 hPa geopotential height (middle panels) and downward surface latent heat flux (lower panels) for the identified European heat events in atmospheric reanalysis as well as low-resolution and high-resolution HighResMIP control-1950 simulations.

8) The predictable coupled atmosphere/Atlantic multidecadal Oscillations and the impact of external forcing [UiB]

One major challenge in climate prediction is identifying predictable signals within the climate system. Building on Omrani et al. (2022), we developed a conceptual oscillatory model to capture the coupled multidecadal atmosphere-ocean variability in the North Atlantic. In this model, the multidecadal strengthening (weakening) of the AMOC and the associated AMV warming (cooling) is driven by positive (negative) NAO phases and regulated by damping timescales of the AMOC and AMV. The ocean (AMV and AMOC) integrates the NAO forcing similarly to Hasselmann's model, which provides positive feedback that amplifies the oscillation.
The negative feedback that reverses its phase is maintained by the impact of the Ocean on the NAO. Using this simple model, we replicated the historical multidecadal evolution of both NAO and AMV (Fig. UiB_1). To further explore this oscillation, we

analysed NorCPM model simulations with no external forcing, all transient external forcings, and volcanic forcing only.

The results of these simulations (Fig. UiB_2c-e) show how internal variability and external forcing influence the coupled NAO-AMOC/AMV oscillation. In the control experiment, the oscillation is driven solely by internal variability. Compared to models with better stratospheric resolution and observations (e.g., Omrani et al. 2022), the NAO and AMV exhibit weaker oscillations, and the AMOC shows low variability. This suggests that the NAO-AMOC feedback is underrepresented in the model. However, the coupled oscillation can exist without external forcing suggesting that the internal dynamics is its first order driver.

In the all-forcing experiment, which includes solar variability, volcanic activity, and greenhouse gases, the oscillation and feedback mechanisms between NAO, AMOC, and AMV are intact, but the period is shorter than in the control. This indicates that external forcings modulates the coupled mode, affecting the timing without fundamentally altering feedback loops. Volcanic forcing, however, amplifies AMOC variability significantly, while NAO and AMV remain weak. This suggests volcanic forcing primarily affects the ocean but fails to fully activate the atmosphere-ocean feedback needed for a robust coupled oscillation.

Mann et al. (2020) argued that the AMV is mainly driven by volcanic forcing using a univariate approach, but this overlooks the coupled dynamics between NAO, AMOC, and AMV. Our results, using a coupled oscillatory approach, show that the oscillation persists without external forcing, highlighting the key role of internal variability in driving multidecadal oscillations. The coupled feedback between atmosphere and ocean is essential for understanding these dynamics, which the univariate approach misses.

Conclusion and Implications for Predictive Skill and the Signal-to-Noise Paradox: The coupled NAO-AMOC-AMV oscillation is mainly driven by internal variability, with external forcing modulating its period and amplitude. The overall magnitude remains weak in our NorCPM model compared to observations and the stratosphere-resolving model in Omrani et al. (2022). This weaker NAO-AMOC coupling reduces the oscillation's amplitude and therefore also the amplitude of the predictable signal, contributing to the reduction of the signal-to-noise ratio and therefore also to the signal-to-noise paradox. The all-forcing experiment shows that external forcing modifies the period of the oscillation but leaves the system too weak to fully take advantage of decadal predictability. Volcanic forcing amplifies AMOC variability but fails to fully trigger the coupled feedback necessary for sustained, predictable oscillations, which limits the model's predictive skill. Enhancing NAO-AMOC coupling and improving stratospheric representation in models could be crucial for improving predictive skill and mitigating the signal-to-noise paradox in decadal climate predictions.

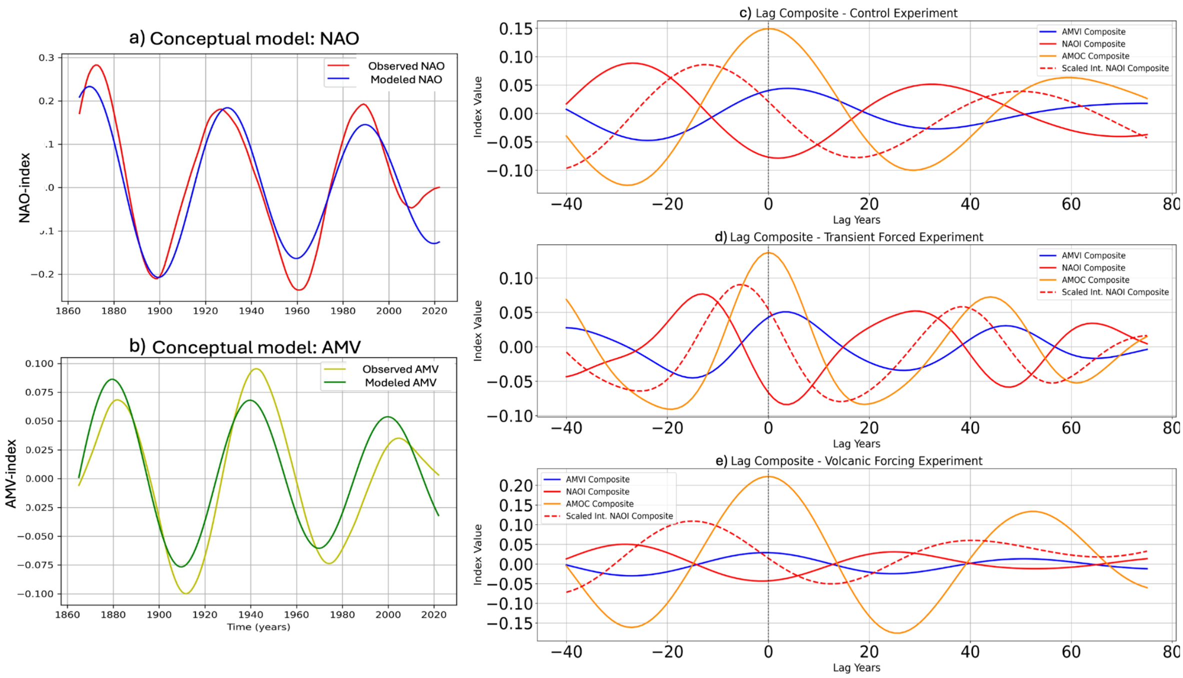

*Figure UiB_1: The multidecadal variability of the NAO-index and AMV-index from the conceptual model compared to their observed values. c), d), and e) represent the lag-composite from the multidecadal atmosphere/ocean coupled oscillation for c) the control simulation, d) the transient forced simulation, and e) the experiment forced only by volcanic forcing. The composite shows the NAO (red), integrated NAO (dashed red), AMV (blue), and AMOC (yellow), and is based on and centered around events with anomalies greater than 1*std of the AMOC index. The coupled oscillation is obtained by applying Multichannel Singular Spectrum Analysis on the coupled atmosphere/ocean system (see Omrani et al. 2022 for details).*

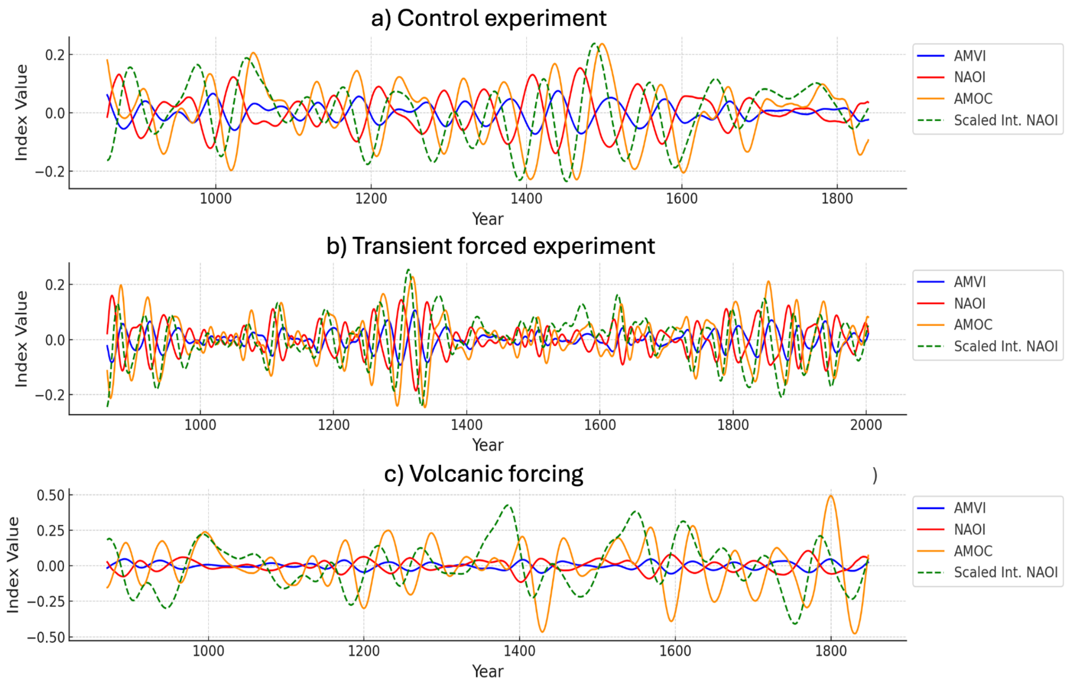

Figure UiB_2 a), b), and c) represent the time series of the reconstructed coupled multidecadal atmosphere-ocean oscillation for a) the control simulation, b) the transient forced simulation, and c) the experiment forced by volcanic forcing only. The coupled oscillation is obtained by applying Multichannel Singular Spectrum Analysis to the coupled atmosphere-ocean system (see Omrani et al. 2022 for details).

9) Impact of Cloud Radiative Effects (CREs) on Wintertime Atmospheric Blocking in the Euro-Atlantic Sector [UiB]

Atmospheric blocking, particularly over the Euro-Atlantic sector, has long been a challenge for climate models, with many underestimating blocking frequency. This study examines the influence of Cloud Radiative Effects (CREs) on blocking formation using the cloud-locking technique in the U.S. DOE's Energy Exascale Earth System Model (E3SM). For understanding the CREs, three experiments were conducted: Control (CTL) with Present-day sea surface temperature (SST) forcing, A cloud-locking experiment (CLOCK) which is identical to CTL, except the cloud properties are "locked" to isolate the interactive CRE. In this CLOCK simulation we prescribed the cloud optical properties from the three years of CTL simulation. We do this by randomly selecting one of the three years of CTL at the frequency of radiative transfer calls made by the atmospheric component of the model. In this way, the CLOCK experiment possesses a nearly identical CRE climatology to CTL, but the CREs are fully decoupled from the dynamics and other physical processes. We also perform a CRE denial experiment, where the long wave CRE (LWCRE) is disabled. In this experiment the mean state also changes.

Key Findings: Blocking frequency is significantly influenced by CREs. Removing interactive CREs in CLOCK reduces blocking frequency by 21.6%, while LWOFF results in a 37.3% reduction compared to CTL (Figure UiB_3). This demonstrates the critical role of CREs in enhancing blocking, with more pronounced effects when longwave cloud-radiation interactions are removed (LWOFF). CREs affect blocking formation by enhancing wave activity through diabatic sources upstream of the block (not shown). This increase in wave activity convergence downstream leads to stronger block formation, particularly in CTL, where interactive CREs are active. In LWOFF, the reduced blocking frequency is associated with decreased low-level baroclinicity and weakened stationary wave ridges.

Identifying Factors Degrading Predictive Skill and Potential for Improvement: Accurate representation of clouds remains a major challenge for models, as they still rely on cloud parameterization. According to this study, this limitation can degrade predictive skill, particularly on seasonal to decadal timescales, by underrepresenting the influence of CREs on blocking events. Transitioning from parameterized clouds to cloud-resolving models could significantly enhance CRE representation, leading to more accurate simulations of blocking and improved model predictions. By better resolving cloud dynamics, these models may capture the cloud-atmosphere interactions that are crucial for blocking formation.

Conclusion and Implications: The study demonstrates that CREs significantly influence blocking frequency and that their accurate representation is essential for improving decadal climate predictions. Moving towards cloud-resolving models could help overcome the limitations of cloud parameterization, improving CRE representation and enhancing the model's ability to simulate atmospheric blocking. These improvements can be important for refining future climate models and reducing the signal-to-noise paradox that currently hampers predictive skill on seasonal to decadal timescales.

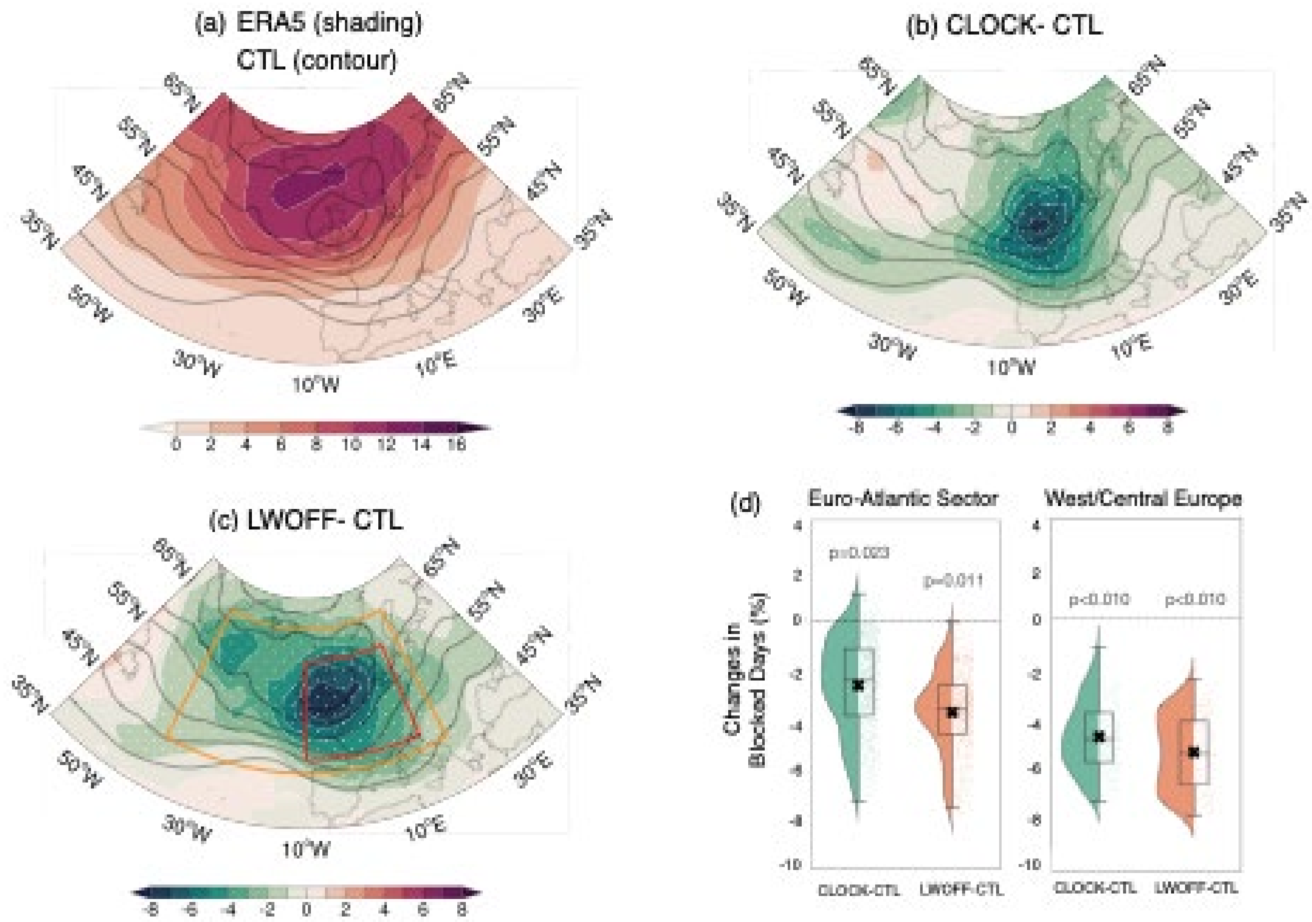

Figure UiB_3: Spatial distribution of Euro-Atlantic winter blocking frequency in the reanalysis and E3SM experiments. (a) Wintertime (December-February) blocking frequency climatology in ERA5 (shading) and CTL simulation (contour lines, with intervals of 2 starting at 2). The unit is percentage of blocked days in the season (i.e., with 2% corresponding approximately to two blocked days per winter). (b) Difference between the CLOCK and CTL (shading) and the climatology in the CTL run (contour lines). (c) Similar to (b) but for the difference between LWOFF and CTL (shading). Dots in (b) and (c) indicate differences exceeding the 95% confidence interval based on the two-tailed t-test. (d) Changes in blocked days averaged over the Euro-Atlantic sector (43◦-65◦N, 40◦W-20◦E; orange box in (c)) and the West/Central Europe (45◦-60◦N, 10◦W-15◦E; red box in (c)) in half-violin-style box-whisker plot. The vertical widths of boxes represent interquartile range, whiskers extend from 5% to 95%, and horizontal lines and x symbols indicate median and mean values, respectively. The dots represent individual data points. The p-values from t-test of CLOCK (LWOFF) and CTL differences are shown in each panel.

10) Response of the Northern Hemisphere stratospheric polar night jet to climate change: Key roles of the tropical oceans and nonconservative effects [UiB]

The stratosphere has a strong impact on surface climate. It plays a crucial role in the response of the Northern Hemisphere to climate change and in the internal decadal-to-multidecadal North Atlantic climate variability, both of which are important for near- to mid-future decadal climate prediction. Understanding the mechanisms and factors controlling the response of the stratospheric polar night jet (SPNJ) to climate change is one of the keys for addressing model discrepancies in simulating and predicting stratospheric circulation and its impact on surface climate over decadal-to-multidecadal timescales. This study explores the role of the ocean, in particular tropical sea surface temperature (SST) changes, finite amplitude wave activity

(FAWA), and non-conservative processes (NCPs)—such as diabatic heating and irreversible mixing—in shaping the response of the Northern Hemisphere SPNJ to future climate change. Using the stratosphere-resolving Atmospheric General Circulation Model (AGCM) MAECHAM5, we investigate how different forcing conditions, such as tropical SST, Arctic sea ice, and extratropical SST, influence the weakening of the SPNJ under projected future climate scenarios.

In this work, we conducted different atmosphere-only experiments: Control Experiment (CTL): Using climatological external forcing, SST, and sea ice (SIC) conditions from 1900-1999, taken from a coupled atmosphere/ocean model simulation. All Forcing Experiment (AFEx): Using projected SST, SIC, and radiative forcings for 2051-2099 (IPCC A1B scenario), taken from a coupled atmosphere/ocean model simulation. Tropical SST-only Experiment (TrSST): Simulated with future tropical SST but present-day climatological external forcing and SIC. Sea Ice-only Experiment (SI-only): Using future sea ice conditions with present-day SST.

Key Findings: The All Forcing Experiment (AFEx) shows that climate change causes a significant weakening of the SPNJ (Fig. UiB_4) that can be explained mainly by the tropical SST (TrSST). This weakening is caused by the interplay between FAWA and non-conservative processes. In both AFEx and TrSST experiments, FAWA enhances the disruption of the SPNJ through large-scale wave propagation (not shown), mainly during the onset of winter (Fig. UiB_4). Non-Conservative Processes (NCPs), such as irreversible diffusive mixing and diabatic heating, also contribute to SPNJ weakening (Fig. UiB_4). These processes become more significant in mid-to-late winter, further reducing the strength of the polar vortex. The response of FAWA and NCPs is strongly maintained by the tropical SST.

Factors Degrading Predictive Skill and Potential for Improvement: Key factor that can degrade the decadal-to-multidecadal predictive skill associated with the SPNJ can be the bias in simulating tropical climatological SST and the SST-responses to climate change. Since tropical SSTs control the response of the polar vortex through their influence on FAWA and NCPs, any bias in tropical SST projections can introduce errors in predicting the polar vortex response to climate change, leading to uncertainties in mid- to long-term climate predictions. It is therefore important to reduce intermodel discrepancies in simulating the tropical SST response to climate change. Correcting tropical SST biases will improve the accuracy of FAWA, NCP, and SPNJ projections.

Conclusion: Tropical SSTs are critical in determining the polar vortex response via FAWA and NCPs. Reducing ongoing intermodel discrepancies in simulating the tropical SST response to climate change will be important in enhancing predictive of SPNJ skill and its impact on the surface related to climate change on decadal to multidecadal timescales.

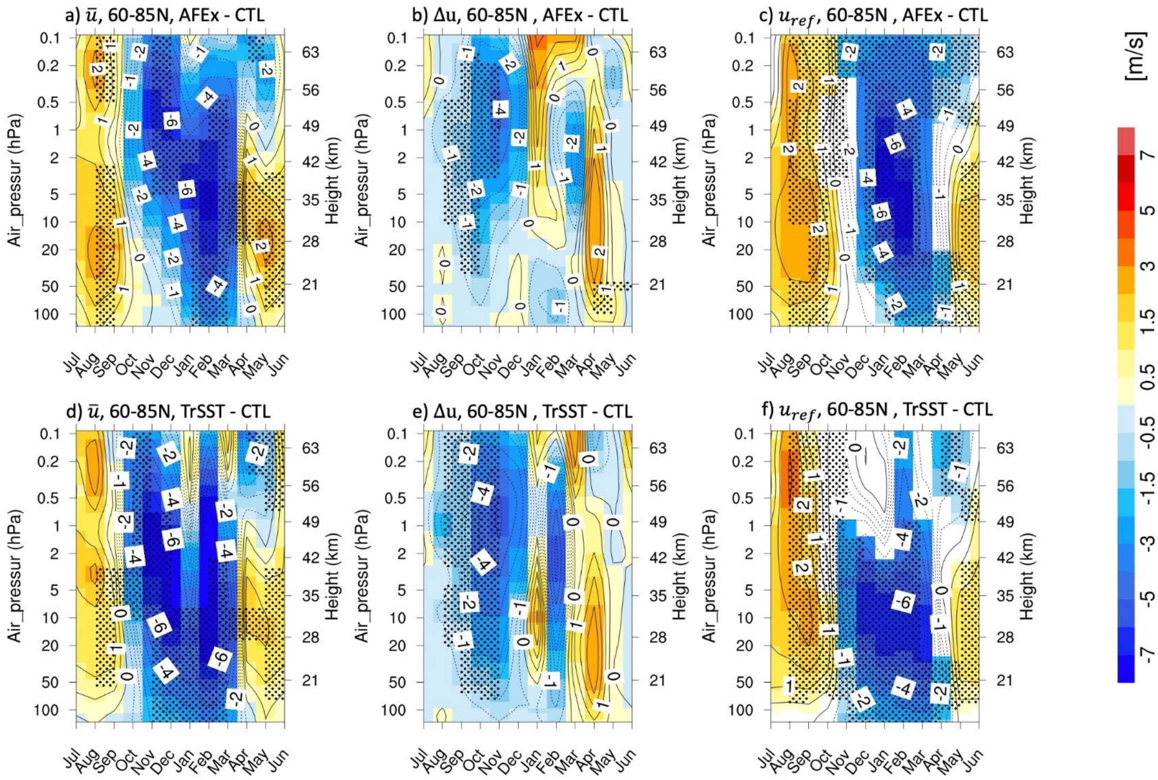

Figure UiB_4: Monthly evolution of the vertical structure of the climatological zonally averaged zonal wind, FAWA-impact and impact of NCPS in response to future climate conditions (in AFEx and TrSST experiments). Simulated climatological monthly evolutions of the vertical structure of the high latitude (60-85N) response in AFEx-experiment of (a) zonally averaged zonal wind (in m/s) and associated contributions to the zonally averaged zonal flow of (b) net contribution of FAWA (in m/s) (c) non-conservative processes (in m/s). (d), (e) and (f) are like (a), (b) and (c) but for the TrSST experiment. Stippling in (a)–(f) indicates the differences exceeding the 95% confidence level based on the two-tailed Students' t-test.

3.3 Status of Knowledge

State-of-the-art climate prediction systems are strongly underconfident in predicting climate variability on seasonal to decadal time scales, especially over land areas and with respect to climate extremes. Consequently, climate predictions on seasonal to decadal time scales are still in need of substantial improvements in order for their outputs to be actionable. Both underestimated signal-to-noise ratio and key mean state biases, such as poorly represented ocean-atmosphere interactions and teleconnections from the tropics, in state-of-the-art climate models have been identified as potential issues degrading predictive skill. There is growing evidence that high-resolution grid configurations, especially resolving meso-scale eddies, can reduce model deficiencies and thus potentially improve predictive skill. However, very high-resolution grid configurations are computationally extremely costly.

3.4 Main Results Achieved

Key results obtained within the framework of this deliverable:

- We analysed the model simulations of observed NAO-temperature teleconnection in several state-of-the-art initialised climate prediction systems. We find that, in particular, over longer forecast periods the initialised predictions struggle to reproduce observed teleconnection patterns which could be one of the reasons contributing to the degradation of added value from initialisation in these prediction systems.
- We have investigated the multi-model differences in predicting the ocean heat content in the North Atlantic region, which we could not explain in terms of differences in key mean state biases due to a corrective (and largely beneficial) effect of initialization. In the Labrador Sea, mean-state biases in the local stratification and surface forcing have been found to potentially explain the differences in representing the predictive skill attributable to external forcings, which is highly uncertain.
- We demonstrated a strong inverse correlation between the NAO and cold surge frequency in Taiwan, with cold surges becoming more frequent during the negative phase of the NAO. This finding is further supported by wave propagation pathway analysis, which reveals that atmospheric waves originating from the North Atlantic impact East Asia's climate through teleconnections. These results underscore the potential of leveraging NAO-based teleconnections to enhance decadal predictions of extreme cold events in East Asia and Taiwan.
- We have developed an adaptation of the MOS method to correct errors in interannual predictions made using the three I4C forecast systems, applied to two specific case studies. This correction method is distinct because it must be tailored to each particular case, and a solid understanding of the underlying physics is essential for the correct selection of predictors for the MLR model associated with MOS. This makes the approach especially valuable for climate services. Our results demonstrate that MOS is effective, as predictions corrected using MOS show greater predictive skill compared to those corrected with the previous WCRP method.
- We show that the MPI-M Grand Ensemble of historical/scenario simulations can - due to a warming background state of the subpolar North Atlantic - reproduce a subpolar marine heat wave, which matches the intensity of the record-strong heat wave observed in the subpolar North Atlantic in summer 2023, within the current decade. This study provides a basis for assessing the predictability of the 2023 subpolar marine heat wave with the MPI-M ocean-eddy resolving climate prediction system.
- We demonstrate that global warming amplifies the internal variability of the summer NAO, which may degrade its predictive skill and increase the risk of associated weather extremes over Europe.
- In collaboration with the University of Kiel, we show that high-resolution model versions improve the simulation of European summer heat waves by reducing

North Atlantic surface biases and thus improving air-sea interactions and better capturing the atmospheric trough and downstream ridge anomalies.

- Using conceptual oscillatory model, we showed that the predictable multidecadal atmosphere-ocean variability in the North Atlantic is a coupled oscillation linking the NAO, AMOC, and AMV. Results show that internal variability is the primary driver of this oscillation, with external forces like solar variability, volcanic activity, and greenhouse gases modulating its period and amplitude. The model highlights volcanic forcing's role in amplifying AMOC variability but indicates that it fails to fully activate atmosphere-ocean feedback for robust oscillation.
- We also showed that CREs significantly enhance blocking frequency in the Euro-Atlantic region, as demonstrated using E3SM with cloud-locking techniques. Removing CREs reduces blocking by up to 37.3%, highlighting their critical role in blocking formation through upstream wave activity. Underrepresentation of CREs in models degrades predictive skill, suggesting that transitioning to cloud-resolving models could improve CRE representation, enhance blocking simulations, and resolve the signal-to-noise paradox in decadal climate predictions.
- We showed how tropical SST changes influence the weakening of the stratospheric polar night jet (SPNJ) under climate change, using the MAECHAM5 model. Results indicate that tropical SSTs drive SPNJ weakening by enhancing finite amplitude wave activity (FAWA) and non-conservative processes (NCPs) like diabatic heating and diffusive mixing. These effects are most significant from mid-to-late winter. The well known Tropical SST biases in models can degrade decadal-to-multidecadal predictive skill associated with global warming, highlighting the need to reduce intermodel discrepancies to improve SPNJ and surface climate projections.

3.5 Progress Beyond State of the Art

This deliverable aims to better understand the factors degrading current climate predictions on seasonal to decadal time scales and thus provides the basis for improved near-term climate predictions, which are more skillful than state-of-the-art ones, in forthcoming deliverables. We have also developed a novel method to better correct drift and systematic errors in climate predictions. This method has the potential to improve the quality of existing state-of-the-art climate predictions on seasonal to decadal time scales, such as those performed within the sixth phase of the Coupled Model Intercomparison Project (CMIP6). Improvements in near-term climate predictions provide important advances to long-standing problems in climate science.

3.6 Discussion and Next Steps

As a first and important step, this deliverable aims to deepen our understanding of the causes of current deficiencies in seasonal to decadal climate predictions. In forthcoming deliverables, we will mitigate these deficiencies by implementing advanced statistical and modelling approaches, such as techniques to subsample ensemble predictions, flux adjustment to correct key surface biases in the mean-state, ocean-eddy-resolving grid configurations and climate predictions with a supermodel consisting of several climate models (D2.2). Based on those approaches showing significant improvements, we will produce a set of new and improved near-term climate predictions to be delivered to the wider prediction community (D2.3).

4 Impact

This deliverable provides the basis to improve climate predictions on time scales (interannual to decadal) at which action must be taken to achieve the European Union's Mission on Adaptation to Climate Change for a climate prepared and resilient Europe by 2030. More reliable and accurate near-term climate predictions, including climate extremes, will lower human, environmental and economic vulnerability to climate impacts and risks, as well as increase the trust in climate predictions, which is key to a successful societal transition. Near-term climate predictions are also expected to be among topics for special interim reports of the Intergovernmental Panel on Climate Change (IPCC).

5 Links Built

- Impetus4Change has organised a workshop on "Climate Prediction and Services over the Atlantic-Arctic region" (hybrid event, May 2024 in Bergen, Norway) together with its sister project Aspect and JPI Oceans / JPI Climate project Roadmap
- MPI-M PhD candidate (Lara Wallberg), jointly supervised by Aspect PI Dr. Wolfgang Müller and Impetus4Change PI Dr. Daniela Matei (PhD defended in November 2023). PhD Thesis results relevant to Task 2.1 have been submitted to Geophysical Research Letters.

6 Communication, Dissemination and Exploitation

6.1 Peer Reviewed Articles

1. Carmo-Costa, T., Bilbao, R., Ortega, P. et al. Trends, variability and predictive skill of the ocean heat content in North Atlantic: an analysis with the EC-Earth3 model. Clim Dyn 58, 1311–1328 (2022)

2. Carmo-Costa, T., Bilbao, R., Robson, J., Teles-Machado, A., and Ortega, P.: A multi-model analysis of the decadal prediction skill for the North Atlantic ocean heat

content, EGUsphere [preprint], https://doi.org/10.5194/egusphere-2024-1569, (2024)

3. Krüger, J., J. Kjellsson, K. Lohmann, D. Matei and R.P. Kedzierski: Improved European heat event simulation by resolving oceanic mesoscale eddies. To be submitted to Nature Communications

4. Liu, Q., J. Bader, J.H. Jungclaus and D. Matei: More extreme summertime North Atlantic Oscillation under climate change. Submitted to Nature Climate Change

5. Lubis, Sandro W., Bryce Haropa, Jian Lua, L. Ruby Leunga, Ziming Chena, Clare Huangb and Nour-Eddine Omrani. Importance of Cloud-Radiative Effects in Wintertime Atmospheric Blocking over the Euro-Atlantic Sector. Submitted to Nature Communication

6. Omrani, Nour-Eddine, Noburo Nakamura, Sandro W. Lubis, Noel Keenlyside and Fumiaki Ogawa· Response of Northern Hemisphere stratospheric polar night jet to climate change: key role of tropical Ocean and nonconservative effects. Submitted to NPJ Climate and Atmospheric Sciences

7. Tsai, C.-T., Y.-C. Wang, W.-L. Tseng*, L.-C. Chiang: Pacific Meridional Mode implicated as a prime driver of decadal summer temperature variation over Taiwan. In revision with Journal of Climate

8. Wallberg, L., L. Suarez-Gutierrez, D. Matei, D. Krieger and W.A. Müller: Extremely warm European summers predicted more accurately by considering sub-decadal North Atlantic Ocean heat accumulation. Submitted to Geophysical Research Letters (joint Aspect - Impetus4Change paper)

6.2 Other Dissemination

Oral and poster presentations

- Emilia Sanchez Gomez, Christophe Cassou, Julien Boe, Remy Bonnet, Pascal Laveau, Yannick Leauté, *A new method for correcting model biases in decadal forecasts*, oral presentation, IMSC2024, Toulouse, June 2024

7 References

1. Bilbao, R., Wild, S., Ortega, P., Acosta-Navarro, J., Arsouze, T., Bretonnière, P.-A., Caron, L.-P., Castrillo, M., Cruz-García, R., Cvijanovic, I., Doblas-Reyes, F. J., Donat, M., Dutra, E., Echevarría, P., Ho, A.-C., Loosveldt-Tomas, S., Moreno-Chamarro, E., Pérez-Zanon, N., Ramos, A., … Vegas-Regidor, J. (2021). Assessment of a full-field initialized decadal climate prediction system with the CMIP6 version of EC-Earth. Earth System Dynamics, 12(1), 173–196. https://doi.org/10.5194/esd-12-173-2021

2. Boer, G.J. et al. (2016): The Decadal Climate Prediction Project (DCPP) contribution to CMIP6. Geoscientific Model Development, 9, 3751–3777, doi:10.5194/gmd-9-3751-2016

3. Kuhlbrodt, T. , R. Swaminathan, P. Ceppi and T. Wilder (2024): A glimpse into the future - The 2023 ocean temperature and sea ice extremes in the context of longer-term climate change. Bulletin of the American Meteorological Society, doi:10.1175/BAMS-D-23-0209.1

4. Smith, D. M., Scaife, A. A., Eade, R., Athanasiadis, P., Bellucci, A., Bethke, I., Bilbao, R., Borchert, L. F., Caron, L.-P., Counillon, F., Danabasoglu, G., Delworth, T., Doblas-Reyes, F. J., Dunstone, N. J., Estella-Perez, V., Flavoni, S., Hermanson, L., Keenlyside, N., Kharin, V., … Zhang, L. (2020). North Atlantic climate far more predictable than models imply. Nature, 583(7818), 796–800. https://doi.org/10.1038/s41586-020-2525-0

IMPETUS4CHANGE (I4C)

IMPROVING NEAR-TERM CLIMATE PREDICTIONS FOR SOCIETAL TRANSFORMATION

Grant agreement ID: 101081555

Call: HORIZON-CL5-2022-D1-02

Type of Action: HORIZON-RIA

Start date: 1 November 2022

Duration: 48 months

Website	impetus4change.eu
Twitter	@I4C_eu
LinkedIn	Impetus4Change
Zenodo repository for I4C open access documents	Impetus4Change Community